UNIVERSITÀ DEGLI STUDI DELL'AQUILA
DIPARTIMENTO DI MEDICINA CLINICA, SANITÀ PUBBLICA, SCIENZE DELLA VITA E DELL'AMBIENTE

DOTTORATO DI RICERCA IN SCIENZE DELLA SALUTE E DELL'AMBIENTE

CURRICULUM IMAGING MOLECOLARE E ULTRASTRUTTURALE

XXXV CICLO

Morpho – functional evaluation and potential application of biomaterials in regenerative therapies: human periodontal ligament fibroblasts in vitro model

SSD BIO/16

Dottoranda

Diana Torge

_____

Coordinatore del corso

Prof. Maria Grazia Cifone

_____

Tutor

Prof. Guido Macchiarelli

_____

Co - tutor

Prof. Serena Bianchi

_____

a.a. 2021/2022

TABLE OF CONTENTS

ABSTRACT **1**

GRAPHICAL ABSTRACT **4**

LIST OF ABBREVIATIONS **5**

CHAPTER 1 - INTRODUCTION **8**

1.1 Principles of tissue regeneration 8

1.2 Triad of Tissue Regeneration 13

1.3 Jawbone regeneration 17

CHAPTER 2 - BIOMATERIALS **21**

2.1 Tissue regeneration and biomaterials 21

2.2 Class of biomaterials 23

2.2.1 Autologous biomaterials 23

2.2.2 Allogenic biomaterials 28

2.2.3 Xenogenic biomaterials 30

2.2.4 Natural and synthetic polymers 31

CHAPTER 3 - AIM OF THE RESEARCH **34**

CHAPTER 4 - MATERIALS AND METHODS **36**

4.1 Evaluation of Different APCs: Morphological and Biological Comparisons and Considerations 38

4.1.1 Sampling Procedures and APC Preparation 38

4.1.2 APC Preparation: L-PRF 38

4.1.3 APC Preparation: CGF 39

4.1.4 APC Preparation: APG 39

4.1.5 Cell Culture 40

4.1.6 Cell Proliferation Assays and Statistical Analysis 40

4.1.7 Morphological Analysis 41

4.1.8 Morphological Analysis: LM 41

4.1.9 Morphological Analysis: SEM 42

4.1.10 Morphological Analysis: CLSM 43

4.2 Bio-Morphological Reaction of hPLFs to Different Types of Dentinal Derivates: In Vitro Study… 44

4.2.1 Sampling Procedures and Dentine Derivates Preparation 44

4.2.2 TT Protocol 45

4.2.3 The Smart Dentine Grinder Protocol 45

4.2.4 Smart Dentine Grinder Protocol Internally Modified 46

4.2.5 Control Material 46

4.2.6 Cell Culture 47

4.2.7 Cell Proliferation Assays and Statistical Analysis 47

4.2.8 Morphological Analysis 48

4.2.9 Morphological Analysis: LM 48

4.2.10 Morphological Analysis: SEM 49

4.2.11 Morphological Analysis: CLSM 50

4.3 Morphological and Biological Evaluations of hPLFs in Contact with Different Bovine Bone Grafts Treated with Low-Temperature Deproteinisation Protocol 52

4.3.1 Biomaterials 52

4.3.2 Cell Culture 53

4.3.3 Cell Proliferation Assay and Statistical Analysis 54

4.3.4 Morphological Analysis 55

4.3.5 Morphological Analysis: LM 55

4.3.6 Morphological Analysis: SEM 56

4.3.7 Morphological Analysis: CLSM 56

CHAPTER 5 - RESULTS 58

5.1 Evaluation of Different APCs: Morphological and Biological Comparisons and Considerations 58

5.1.1 Cell Proliferation Assays and Statistical Analysis 58

5.1.2 Morphological Analysis: LM 60

5.1.3 Morphological Analysis: SEM 62

5.1.4 Morphological Analysis: CLSM 63

5.2 Bio-Morphological Reaction of hPLFs to Different Types of Dentinal Derivates: In Vitro Study… 66

5.2.1 Cell Proliferation Assays and Statistical Analysis 66

5.2.2 Morphological Analysis: LM 70

5.2.3 Morphological Analysis: SEM 72

5.2.4 Morphological Analysis: CLSM 75

5.3 Morphological and Biological Evaluations of hPLFs in Contact with Different Bovine Bone Grafts Treated with Low-Temperature Deproteinisation Protocol 77

5.3.1 Proliferation Assay 77

5.3.2 Morphological Analysis: LM 79

5.3.3 Morphological Analysis: SEM 80

5.3.4 Morphological Analysis: CLSM 82

CHAPTER 6 - DISCUSSION 84

CHAPTER 7 - CONCLUSIONS 101

References 103

Appendix 118

ABSTRACT

Regenerative procedures in oral and maxillofacial surgeries are still a challenge for researchers and clinicians. Understanding the biological and morphological reaction of human cells toward regenerative biomaterials is essential to choose the most performing biomaterials for specific clinical situations. This research project aims to investigate the biological and morphological reaction of hPLFs toward different classes of biomaterials: respectively, APCs, dentinal derivates, and DBBM. The first study provided a biological and morphological analysis of APCs obtained with different protocols, in culture with hPLFs in standard conditions (37° C - 5 % CO_2). The study design included the evaluation of L-PRF, CGF, and APG in contact with the hPLF cell line after 24 h, 72 h and 7 days of in vitro culture. Subsequently, hPLFs were cultured in standard conditions in contact with different dentinal derivates (TT, DDP, SG, and BIOS) and the evaluations were performed after 24 h, 72 h, and 7 days of in vitro culture. Finally, this research project also provides a biological and morphological evaluation of hPLFs cultures in contact with different DBBM particles, treated with a low-temperature protocol, by performing the bio-morphological evaluations after 24 h, 72 h, and 7 days of in vitro culture.

The presented three studies shared a similar experimental design: in fact, the biological reaction of hPLFs towards these different classes of biomaterials was evaluated by XTT assays to assess cell proliferation and viability. Furthermore, the morphological reaction was evaluated by LM, SEM, and CLSM examinations.

As regards APCs, the XTT assay showed an interesting response in the growth curve towards CGF. This biological data was confirmed by LM and SEM evidence, with the best results for the CGF and L-PRF. Moreover, dentinal derivates (SG, DDP, and TT) induced in hPLFs a significant growth, as suggested by XTT assays. Morphological evidence confirmed this biological data: densely packed cells, characterized by a modified shape, cytoplasmatic extensions (DDP and TT) and the thickening of the cellular membrane (SG and BIOS) were respectively detected by LM and SEM. Furthermore, CLSM detected a progressive increase and a dynamic expression of proliferative and cytoskeletal markers (vinculin, actin, and integrin), suggesting a cytoskeletal reaction to the tested biomaterials. Regarding DBBM, the XTT assays showed a proliferation growth curve in different DBBM particles treated with a low-temperature protocol, with a statistical significance between the different experimental materials and the negative control. Morphological observations highlighted significant

morphological changes in hPLFs, characterized by a polygonal shape (LM), surface reactions with the thickening of the membrane (SEM), and expression of actin (CLSM). In conclusion, a significant onset of the growth characterized the hPLFs exposed to the selected classes of biomaterials, making them promising options for periodontal regeneration interventions.

GRAPHICAL ABSTRACT

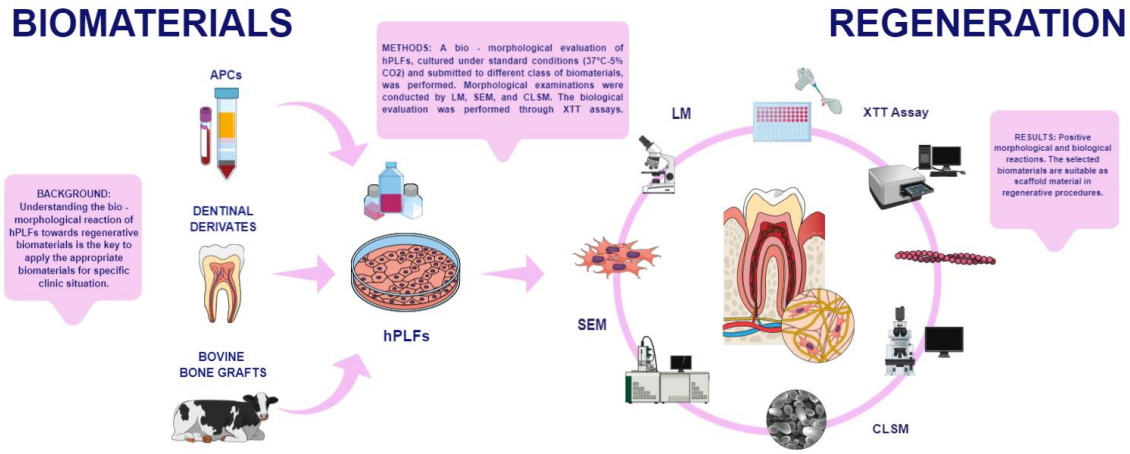

LIST OF ABBREVIATIONS

AA	Augmented Area
APCs	Autologous platelet concentrates
APG	Autologous platelet gel
BIOS	Deproteinized bovine bone
BMPs	Bone morphogenetic proteins
BSA	Bovine serum albumin
CBA	Cryopreserved bone allograft
CGF	Concentrated growth factors
CLSM	Confocal laser scanning microscopy
DAMPs	Damage – associated molecular signals
DAPI	4',6 - Diamidino - 2 - Phenylindole
DBBM	Deproteinised bovine bone mineral
DBM	Demineralized bone matrix
DDP	Deproteinized and demineralized dentine
DPBS	Dulbecco's phosphate buffered solution
ECM	Extracellular matrix
EGF	Epidermal - growth factor
FBS	Fetal bovine serum
FDBA	Freeze - dried bone allografts
FFBA	Fresh frozen bone allografts
FGF	Fibroblast growth factor
FGS	Fibroblast growth supplement
FM	Fibroblast Medium
GBR	Guided bone regeneration
HA	Hydroxyapatite
HDMS	Hexamethyldisilane
HEMA	Hydroxyethyl methacrylate
hPLFs	Human periodontal ligament fibroblasts

HSP	Heat shock protein
IGF	Insulin-like growth factor
IL - 1α	Interleukin -1α
IL - 1β	Interleukin -1β
IL - 1R	Interleukin -1 receptor
IL - 6	Interleukin - 6
IL - 33	Interleukin - 33
ILGF - 1	Insulin-like growth factor -1
LM	Light microscopy
L - PRF	Leukocyte - platelet rich fibrin
MBA	Mineralized bone allografts
MPBA	Processed mineralized bone allografts
MSA	Maxillary sinus lift technique
mtDNA	Mitochondrial DNA
NaOCl	Sodium hypochlorite
NaOH	Sodium hydroxide
NF-kB	Nuclear factor kappa B
PBS	Phosphate buffered solution
PDGF	Platelet - derived growth factor
PFA	Paraformaldehyde
PMMA	Polymethyl methacrylate
PRF	Platelet - rich fibrin
PRGF	Growth factor - rich plasma
PRP	Platelet - rich plasma
RT	Room temperature
SEM	Scanning electron microscopy
TCP	Tricalcium phosphates
TGF - β	Transforming growth factor - β
TLRs	Toll - like receptors
TNF - α	Tumor necrosis factor - α

TT	Tooth – transformer
VEGF	Vascular endothelial growth factor
WHO	World Health Organization

CHAPTER 1 - INTRODUCTION

1.1 Principles of tissue regeneration

Tissue regeneration is a body response to trauma or injury. This phenomenon is characterized by the activation of a cascade of cellular, molecular, and biochemical processes, which lead to tissue repair [1].

Regenerative procedures have received much interest in recent decades due to the demand for restoration and regeneration techniques of missing tissues and organs [2].

Regenerative medicine requires a triad of physiologically active cells, substrates, and biomolecules, which trigger and sustain tissue repair [3]. The idea of tissue regeneration has persisted throughout history until it became a reality in the early 1900s, when scientist Alexis Carrel discovered the technique of cell culture [4]. Cells, scaffolds, and growth-stimulating signals are key components of the tissue engineering triad, as they interplay to form a new tissue [4,5]. The regeneration process begins with the synthesis of a scaffold, within there are cellular populations in contact with growth factors [4]. Other methods involve the use of an existing scaffold: for example, the use of cells deriving from a donor organ, whose collagen scaffold is applied to generate new tissue. This innovative approach uses human tissue scaffolds left over from surgery, in contact with

the patient's cells, aiming to recreate personalized organs, not rejected by the immune system [3].

Regenerative medicine shows a multidisciplinary profile based on the application of allogeneic or autologous cells, scaffolding biomaterials, genetic modifications, and molecular signals, which contribute, alone or in combination, to repair, regenerate, or replace dysfunctional cells, tissues, or organs, through an integrated work plan [7]. Stem cells and derived products are the signature active ingredients applied in regenerative regimens, to form de novo tissue or promote innate repair [6]. Furthermore, advances in materials science and biotechnology offer complementary perspectives for growing tissue bio-grafts and whole organ engineering.

Moreover, as an emerging field in health sciences, tissue regeneration also provides a significant starting point for the treatment of various pathological conditions. Regenerative technologies are in fact interdisciplinary and transformative practices, offering a disruptive armory that aims at the normative restoration of pathological organs and tissues and promotes their healing [6]. Complete regeneration promotes the restitutio ad integrum of the damaged tissue or organ.

In contrast, incomplete tissue regeneration promotes tissue mass loss or replacement with fibrotic scars associated with impaired functional recovery [8]. Specifically, tissue damage is followed by a massive immune response, which provides instant defense against potential pathogens, that invade the damaged tissue [9]. Furthermore, the adaptive immune response also plays a considerable role in tissue regeneration [9], with the aim to sustain the repair process [10].

Tissue regeneration consists of three phases: hemostasis and inflammation, a proliferative phase with the neoformation of new tissues, and tissue remodeling. Hemostasis and platelet aggregation are followed by wound infiltration with lymphocytes, phagocytes, and cells involved in the subsequent proliferative phases. The main features of tissue remodeling are: increased remodeling and turnover (synthesis, deposition, remodeling, and degradation) of ECM molecules and loss of excess cell types by apoptosis [11]. Besides, cell-cell and cell-matrix interactions, along with a proper balance of soluble molecular mediators, are vital for adequate wound healing in all three phases [11]. Molecular factors underlying the tissue regeneration process are: the induction of local inflammation in response to DAMPs and molecular signals, associated with pathogens.

Among DAMPs, HSP, monosodium urate, extracellular ATP, and nucleic acids, with specific attention to mtDNA, play a key role in the process [9].

Additionally, reminders of ECM components such as hyaluronic acid, collagen, elastin, fibronectin, and laminin stimulate the inflammation [9]. TLRs and other types of receptors recognize danger signals and trigger inflammation via the activation of NF-κB transcription factors or interferon regulatory factors [9]. TLRs activate tissue-resident macrophages and induce the expression of pro-inflammatory cytokines such as TNF-α, IL-1β, and IL-6 [9]. However, the dominant danger signal varies in the injury context, including the location, extent, mode of cell death, and time after injury [9]. Overall, warning signs significantly affect the healing process in the early stages. Indeed, they are required to trigger and sustain inflammatory dynamics, with a considerable impact on the regenerative process [10].

Among the human tissues, bone tissue has a significative regenerative potential, as it can repair itself in response to trauma or injury. However, if the lesion exceeds a specific size, bone synthesis is more complicated, requiring surgery [1]. In cases of loss of an important quantity of tissue, there are numerous therapeutic strategies, which promote the regeneration of bone tissue: a widespread approach is the transplantation of healthy

autogenous tissues or allografts [1]. The application of bone grafts, whether autologous or performed with biomaterials, and techniques of GBR, with membranes capable of exerting a curtain effect, are able to trigger regeneration processes in the intervention site, capable of recreating a lost portion of tissue, thus restoring both the anatomy and function of the bone site [3]. Transplantation of healthy autogenous tissue is widely used in bone grafts, while allograft is more required for the reconstruction of whole organs, such as the liver, kidney, and heart [1]. However, there are numerous issues associated with this type of intervention: for autogenous grafts, the morbidity of the tissues and the donor site can be a problem; for allografts however, immune complications and the availability of a donor are still a significant challenge [1]. For these reasons, it is important to develop new or synthetic bioengineered bone graft substitutes.

Moreover, bone regeneration also involves periodontal tissues, often affected by environmental issues, pathogenic microorganisms, and genetic dynamics, which lead to periodontitis and bone loss. Forefront techniques have been developed to enhance the osteogenesis process, including bone grafts, scaffolds, stem cells, and growth factors [12]. Firstly, autogenous bone grafts are viewed as the "gold standard" for bone replacement [13]. Secondly, tissue banks provide different types of allogeneic bone grafts [14],

including FDBA and freeze-dried demineralized bone allografts. Thirdly, xenografts were used, such as Bio-Oss: for example, different studies investigated the effects of titanium mesh in combination with Bio-Oss, for localized alveolar ridge augmentation [15]. Fourth, synthetic alloplastic materials have been developed: among them, HA, TCP, a calcium layer polymer of PMMA and HEMA polymer [16], and bioactive glass. Recent scientific advances in biomaterials and cell therapies have significantly contributed to the development of engineered tissues for bone regenerative purposes.

1.2 Triad of Tissue Regeneration

From a biological point of view, tissue regeneration requires three fundamental components: a scaffold, capable of providing a structure and a substrate for cell growth and development; a cellular population, which facilitates tissue genesis, and growth factors, biophysical stimuli which regulate the growth and differentiation of the cell population within the scaffold [1]. These three elements constitute the tissue triad, necessary to support the tissue regeneration process in temporally interconnected phases. Bone regeneration occurs through three mechanisms: osteogenesis, osteoinduction, and osteoconduction (Figure 1). Osteogenesis is the formation and development of bone and

occurs also in absence of undifferentiated mesenchymal stem cells. Osteoinduction is the transformation of undifferentiated mesenchymal stem cells into osteoblasts or chondroblasts through growth factors that exist only in living bone. Osteoconduction is the process that provides a bio-inert scaffold, or physical matrix, suitable for the deposition of new bone from surrounding bone or to encourage the growth of differentiated mesenchymal cells along the graft surface [4]. The scaffold consists of the material (autologous or otherwise), which is grafted to restore the bone defect.

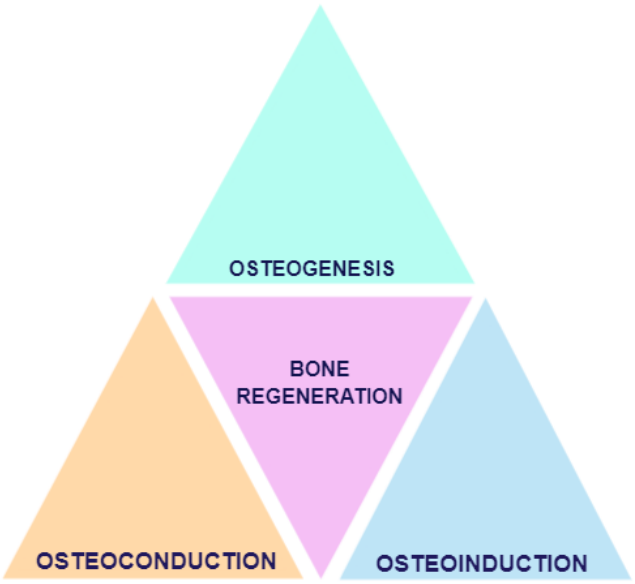

Figure 1. The three properties fundamental for bone regeneration. *The osteoconduction, induced by the scaffold network, which allows the migration of the cells. Osteoinduction instead is promoted by growth factors, which determine the cellular proliferation. Finally, osteogenesis characterized by the synthesis of new bone tissue, through osteoblasts.*

Scaffolds create a spatial structure capable of hosting and mechanically supporting the cellular and tissue elements (e.g., blood vessels), which will colonize and regenerate the grafted volume. This function is crucial, as the diffusion of cells and vessels is impossible in an empty space. The graft thus performs the first important effect of osteoconduction, by acting as a physical space, which can be colonized by cells and vessels to which it gives mechanical support [3]. The osteoconductive effect does not envisage a biochemical interaction between the graft and the recipient tissue. However, it exclusively depends on the physical parameters that characterize the biomaterial: its morphological and surface characteristics (such as the size of the pores, the surface roughness, and others). In the case of autologous bone grafts, these parameters being the same tissue being regenerated are clearly already optimal [3]. Cellular elements are responsible for the regenerative event: in the bone tissue, osteoblasts lay down the new bone matrix, part of which will subsequently be mineralized. In conventional regenerative techniques, the cells reach the area where the new tissue is to be generated, migrating from the periphery to the site to be regenerated. As regards autologous bone grafts, a part of the osteoblasts, compatibly with the degree of necrosis of the graft due to the duration of the ischemia generated by the act of sampling, will also be brought to the site of the graft with the autologous tissue

itself [3]. The third element necessary for bone regeneration, is growth factors, chemical signals of a peptidic nature, which trigger and modulate the various processes which underlie bone regeneration [1]. Growth factors play a fundamental role also in cell migration, modulating cellular activity and providing the stimulus to cells to differentiate and produce matrix for tissue development. They also stimulate the production of angiogenic signals, inducing the formation of a new vascular network essential for the functioning of cells, as a source of nutrients and oxygen [4]. Growth factors exert their functions through significant variations of their local concentration, not only in relation to their absence or presence [1]. Growth factors reach the grafted site coming from the patient's vital tissue: they can be carried by the bloodstream and synthesized and secreted by cellular elements (also carried by the bloodstream or present at the recipient bone bed). Finally, they are also responsible for the osteoinduction effect, that will lead to the regeneration of the bone tissue.

In the case of autologous bone grafts, a small part of these factors is already present in the graft itself, even if the variation in concentration capable of "igniting" the regenerative events is due to the local contribution of the recipient tissue. Growth factors' influence on target cells is not only performed by activating and binding with a specific receptor,

specific intracellular events (switching on or off genes, up- or down-regulation of specific biochemical pathways, etc.), but also recalling the same cellular elements in the site to be regenerated by chemotaxis [1]. For these reasons, the use of growth factors provides cellular modulation in the area of interest: instead of completely depending on the capacity of the host organism's cells, for the regeneration of new tissue and the production of growth factors, stimulates cell proliferation [1].

1.3 Jawbone regeneration

Besides, in the field of regenerative medicine, great interest is reserved to the regeneration of jawbone, whose biomorphology differs from the bone physiology of the skeletal system, form a histological, anatomical and physiological point of view [17,18]. Jawbone's differences are associated to specific functional roles, associated to the anatomic region they belong: the oral cavity. Firstly, a masticatory function, due to the articulation of the alveolar bone with the teeth and also phonatory, respiratory, sensory and physiognomic roles [18,19].

Since the alveolar processes are considered portion articulating with the teeth, diseases involving one influence the health of the other. Indeed, infective, inflammatory, and traumatic pathologies can affect the teeth and the alveolar bone, leading to resorption,

especially when the dental element is lost. Moreover, dental tissues' pathologies are strongly linked to tooth loss, by inducing important inflammatory sequelae, such as periodontitis and traumas, which significantly compromise the degree of bone loss around the tooth [18,19].

Current therapies to restore jaw and craniofacial defects, might include multiple surgeries, firstly to reconstruct the alveolar bone defects and secondly to place dental implants, after the jawbone defect has healed, a procedure which requires up to 3-6 months, before full restoration of functionality [6]. Indeed, an adequate bone quantity and quality are essential for the success of implant therapy [20]. The posterior edentulous maxilla and the posterior mandibular presents unique challenges for implant placement. The most important of these is the presence of the maxillary sinus. Tooth extraction is often followed by pneumatization of the maxillary sinus and resorption of the alveolar ridge [21].

Posterior maxilla rehabilitation depends on the amount of bone present under the sinus. Implant placement and prosthetic rehabilitation of the posterior maxilla can be challenging, due to maxillary alveolar atrophy after tooth extractions and pneumatization of the maxillary sinus. Sinus floor augmentation (i.e., maxillary sinus augmentation), first

described by Boyne and James, subsequently by Tatum, and modified by many others, is a conventional procedure with low complication and failure rates. The main objective of alveolar bone graft surgery is to facilitate the natural regenerative process of bone and restore an optimal functional state, through the synergistic combination of bone graft materials, cells, and growth factors [21].

The maxillary bone represents a difficult area to manage, due to a low level of mineralization, alveolar bone atrophy and pneumatization of the maxillary sinus. MSA technique has been applied since the 1970s and involves placing bone grafts in the maxillary sinus floor to increase bone volume and density, with good long-term efficacy [22,23]. Ideally, bone grow occurs in the AA, thus increasing bone supply and stability for dental implants [24]. Furthermore, edentulous posterior mandible represents a considerable challenge in the rehabilitation of prosthetic implants [25]. The mandibular vertical bone augmentation procedures are highly susceptive to infection and postoperative complications, due to their intrinsic nature and high microbial load in the oral cavity; at the same time, they are uncomfortable for the patient. The success of mandibular vertical ridge augmentation depends on the operator's clinical skill and experience, but also from the anatomical difficulties of the atrophic alveolar site. For these

reasons, the vertical ridge augmentation is difficult to perform. Anyway, the application of a specific protocol, and improvement of the bone – implant contact surface might provide predictable results [25].

Numerous materials for bone grafting have been used in this technique: autologous bone, allograft and xenograft, biomaterials characterized by specific osteogenic properties (osteoconductivity, osteogenesis, osteoinductivity). While autografts comprise numerous growth factors and autologous cells, which can directly exert their osteoinductive potential in the host tissue, xenografts can promote cell adhesion, proliferate, differentiate, and deposit new bone. Furthermore, grafts of bovine origin have been used, by virtue of a great biocompatibility, osteoconductivity and stability, to respond to the demands of regenerative medicine [26].

CHAPTER 2 - BIOMATERIALS

2.1 Tissue regeneration and biomaterials

Biomaterials are a class of materials, characterized by specific chemical, mechanical and biological properties, which make them suitable and safe for contact with living tissues [27]. Regarding their application, the early seventies saw the conception of a second generation of materials, defined as "biomedical materials". Scientific research applied these biomaterials since 1980, leading to the evolution of biocompatible and multifunctional biomaterials, characterized by cytocompatibility and bioactivity, understood as the ability to interact with the tissue environment, activating a specific biological response. This has led to the experimentation of bioactive biomaterials, for dentistry or for tissue reconstruction in orthopedics [28]. Different solutions were evaluated, including ceramics, glass ceramics and composites, while in 1990 experiments were conducted on synthetic HA, a biomaterial characterized by osteoconductive properties [29]. This biomaterial had a wide application, specifically to guide the reintegration of bone tissue [29–31]. Essential function associated with these biomaterials is biocompatibility, a key function together with mechanical resistance [27].

Furthermore, the biomaterial should also show a significative bioactivity and bioadsorbability [32,33]: among them, magnesium [34], zinc [35], copolymers of polyglycolic acid - polyactic acid and calcium phosphate [36,37] are bio-absorbable and biodegradable. The evolution of biomaterials had a significant impact on medicine, however there are still many challenges to be faced, to which biomaterials could contribute, such as sustainability, new regulamentation [38] and the continuous innovation technology. In fact, if the application of bioactive and resorbable biomaterials has improved tissue implants, however these implants are not exempt from revision surgery, often increasing healthcare costs. In conclusion, the evolution of biomaterials proved a critical understanding of the future and ideal characteristics of these tools fundamental, to conceive functional solutions and establish efficient standards, necessary for the assessment of emerging biomaterials [39,40].

2.2 Class of biomaterials

In the last decade, tissue regeneration procedures have received great interest, due to an increased demand for organ and tissue regeneration techniques, in the most disparate fields. In dental field, for example, various techniques have been proposed, aimed at increasing the bone or soft tissue around the tooth, implants, or for prosthetic rehabilitation [41–43].

2.2.1 Autologous biomaterials

Autologous biomaterials represent the choice of choice for the treatment of periodontal defects and bone regeneration, due to their osteoconductive, osteoinductive and osteogenic properties [44,45]. Osteoconduction depends by the scaffolds, which represent the structure, which allow cell replication and tissue development. Osteogenic properties are due to the presence of osteoblasts, which produce the extracellular matrices, while osteoinduction is stimulated by growth factors initiating a series of events, which lead to the regeneration process [46]. The autologous bone is harvested from a site of the same patient: specifically, both from extra-oral (iliac crest, tibial bone) and intra-oral sites (mandibular ramus, symphysis of the chin and maxillary tuber) [47]. This class of biomaterial possesses all three properties required for regeneration: the bone structure in

fact acts as a physical support for osteoconduction, as a real scaffold. The morphology of the cortical graft is optimal for mechanically supporting which will be colonized by the cellular elements [48]. Furthermore, autologous biomaterials have a remarkable distribution of viable osteoblasts, which represent the portion of material for osteogenesis, necessary for cell proliferation and production of new bone tissue in the recipient sites [49]. Finally, vascular supply of the recipient sites and the harvested biomaterial provide the growth factors needed for osteoinduction [50]. Biocompatibility, osteoinduction and regenerative potential represent the most important feature of this class of biomaterials. Possessing all these properties and belonging to the same patient, autologous bone is the gold standard material in bone regeneration procedures, by virtue of the unlikely risks of transmitted diseases and the absence of immunological reactions [48]. However, a limiting factor for the use of such biomaterials is the scarce availability: the harvesting of autologous bone graft requires a secondary surgical site (i.e., a donor site), increasing the post-operative discomfort of the patient [45,51]. To this aim, alternative solutions have been proposed: allogenic, xenogenic and synthetic biomaterials [52]. In the wide family of autologous biomaterials, a primary role is reserved to autologous platelet concentrates, used by clinicians as a "natural scaffold", thanks to the fibrin fiber network, or in

combination with other biomaterials, due to their evident osteoconductive and osteoinductive properties [53]. In recent years, different protocols have been proposed to obtain autologous platelet concentrates: the first was PRP and PRGF protocol [54]. Anyway, the preparation of a material, rich in growth factors, is complex, limiting its use: according to this protocol, blood, taken by venipuncture in test tubes with citrate acid dextrose, was subjected to a first centrifugation [55]. Factors limiting use and versatility of PRP and PRGF enhanced the development of a second generation of APCs: PRF [56]. Protocols used for PRF preparation are simpler than PRP ones, with no need for biochemical manipulation of the blood. PRF preparation in fact includes the use of a centrifuge (the original protocol proposed by Choukroun et al. provided for a centrifugation at a speed of 3000 rpm for 10 min), giving a different quality to the polymerized fibrin [57], when compared to PRP.

CGF, which derived from PRF, contain high levels of growth factors, due to their high-density tetramolecular matrix fibrin [58]. The main advantage of using CGF in regenerative procedures is the slow release of growth factors, which improves the healing process [59]. Autologous platelet concentrates are used as a biomaterial in regenerative dentistry, given the presence of fibrin fibers and the high content of growth factors: the

fibrin obtained is a three-dimensional matrix, in which platelets, glycan chains and cytokines, structural glycoproteins are trapped, which constitute a network suitable for cell growth and represent the osteoconductive scaffold [60]. Growth factors, activated by the polymerization of the blood clot and stimulated by their own regeneration properties, increase the reparative mechanism in wound healing processes. Major growth factors, released from autologous platelet concentrates are: PDGF, TGF-β, IGF, EGF, FGF and BMPs [50]. PDGF stimulates cell proliferation and collagen synthesis in fibroblasts; TGF-β induces the expression of extracellular matrix proteins, affects osteoblasts at an early stage of development and simulates collagen synthesis by fibroblasts; IGF aids in differentiation and stimulates osteoblast proliferation and differentiated functions, such as type I collagen expression [50]. BMPs are a family of signaling molecules, which promote new bone formation, even at heterotopic sites. Specifically, autologous platelet concentrates contain BMP-2, which can induce osteoblast differentiation [61]. These growth factors contribute to the osteoinductive potential, which characterizes this class of biomaterials. Another autologous material, used for alveolar bone regeneration, is dentin and its derivatives [62]. Tissue more readily available in dental practice, compared to blood or bone taken from other sites, dentin is very close to bone tissue by chemical

composition and embryological origin [63]. Dentin is composed of a mineral phase (70%), an organic matrix (20%), water (10%) and the tubule of odontoblasts, which derive embryologically from a mesenchymal tissue [64]. The mineral phase of dentin is made up of calcium phosphate molecules, in four different forms (amorphous calcium phosphate, HA, tricalcium phosphate and octacalcium phosphate); the organic matrix is instead made up of collagen I fibers and proteins such as growth factors, including bone morphogenetic proteins [64]. Due to this composition, dentin is considered a valid grafting material; moreover, it is a mineralized tissue, so it is possible to obtain three forms of graft material, which can be used for regenerative purposes: the mineralized dentin matrix, the partially demineralized dentin matrix, and the demineralized dentin matrix [65]. The mineralized dentin matrix provides a stable scaffold, characterized by significant osteoconductive properties, but low osteoinductive potential. The demineralization of the dentin matrix, using a 2% solution of HNO_3 [65], makes this material suitable for osteoinduction, with a low osteoconductive property. Similar to platelet concentrates, since dentin lacks cell bodies, this autologous biomaterial has no osteogenic properties.

2.2.2 Allogenic biomaterials

Allografts are bone grafts, derived from an individual of the same species. Most allografts are osteoconductive, as they provide a scaffold, which allows clots to grow, stabilize, promote revascularization, facilitate host cell repopulation, thereby promoting new bone formation [66]. They are characterized by a remarkable osteoconduction, osteoinduction and unlimited availability, but the main limiting factor is biocompatibility, as well as the ability to transmit diseases (HIV and spongiform encephalopathy) [67]. In general, allogeneic bone grafts are thought to have osteoconductive effects, while osteoinduction is still under investigation and depends on the processing of the allograft [68]. Indeed, there are significant differences between FFBA and further processed allografts. In fact, FDBA, MBA, MPBA, DFDBA, DBM, and CBA [69]. While high complication and failure rates are reported for FFBAs, the application of processed allografts are often associated with a high potential for osteogenic regeneration, natural bone remodeling events, revascularization of regenerated areas, and absence of body reactions, as confirmed by histological and immunohistochemical evaluations [70].

Although allogeneic biomaterials can be considered safe, DNA, cellular debris within the lacunae of osteocytes, and remnants of former intra-trabecular adipose tissue were found

in several allogeneic specimens [70]. It is unclear whether DNA and cells have biological activity, affecting the recipient in the long term. Allogeneic bone grafts have been widely used and are an attractive alternative to autologous bone, as they do not require a donor site or abundant supply; at the same time, they show variable regenerative abilities due to the absence of information about the donor's condition (eg, age and systemic health) [71,72]. The availability of allogeneic bone is virtually unlimited and can be obtained in many sizes and shapes (e.g., powder, injectable forms). Allogeneic bone has an open, porous, and reticulated physical structure like that of autogenous bone, conducive to vascularization of the bone after implantation [73]. Furthermore, allogeneic bone grafts show the same bone healing capabilities as autologous grafts, but although they are mainly used in powder form, they show a lack of versatility and/or ease of handling [74], in specific situations, related to pre-implant surgery, such as sinus floor elevation, guided bone regeneration in horizontal/vertical augmentation, and socket preservation. In summary, the lack of versatility and adaptability limits its use in uneven or hard-to-reach areas.

2.2.3 Xenogenic biomaterials

Xenogenic biomaterials, also known as xenografts, are most used and widespread for oral regeneration, specifically periodontal, peri-implant and bone, due to their osteoconductive properties [75]. These xenografts derived from other species and can be of bovine, porcine or equine origin [52]. The mechanical and compositional properties of the xenogenic scaffold material [76], depend on the age of the animal, from which the tissue is taken. Besides, there is no evidence of zoonotic infections, following xenogenic transplants of whole organs or tissues. Even if autogenous bone is unique in its osteogenic, osteoconductive, and osteoinductive properties, however, it has disadvantages, including a high resorption rate, associated morbidity, and the need for a second donor site. This prompts researchers to look for bone substitutes that overcome these problems. Xenotransplantation is among the most relevant candidates. In fact, a specific commercial xenograft derived from bovine bone, Bio-Oss® (Geistlich Pharma AG, Wolhusen, Switzerland) (ABB), is the most studied and scientifically documented biomaterial for bone regeneration currently available [77]. Xenogenic biomaterials consist of extracellular matrix or individual components of the extracellular matrix. ECM composition and ultrastructure affects the phenotype of the resident cells, biochemical

environment, mechanical forces, and oxygen concentration [78]. Moreover, xenogenic biological scaffolds have historically been classified as medical devices by the FDA and must meet the requirements for a medical device. The device must meet a level of sterility, appropriate for the given application. Patient-related considerations for the use of xenogenic biomaterials should be considered prior to use [78].

2.2.4 Natural and synthetic polymers

Tissue regeneration applies cells, biomaterials, and growth factors to renew or replace damaged tissues. Biomaterials for regenerative purposes include three-dimensional (3D) porous scaffolds, used as grafts to promote the regenerative process. Three types of materials are used in the production of 3D scaffolds: ceramics, synthetic polymers, and natural polymers [79]. Among them, marine coral is a natural bioceramic, characterized by porosity and high compressive stiffness and used as a graft for bone regeneration. This natural bioceramic showed a long evolutionary history of synthetizing genes and proteins, involved in biomineralization, and also expresses BMP2/4 orthologs, suggestive of the presence of skeletal proteins in its tissue.

Moreover, marine coral also presents significant regenerative properties, promoting rapid skeletal repair. For these reasons, they are often applied as a scaffold material for graft

procedures [80]. Alternative biomaterials used as scaffold, and biodegradable polymers also show great regenerative potential due to their biocompatibility and biodegradability [81]. These polymers also present excellent plasticity and are characterized by flexible chemical structures [82]. However, different natural polymers are suitable for soft tissue, but they difficulty match the stiffness and stability of bone tissues: for these reasons, combining natural polymers and synthetic ones, but also compounding organic and inorganic materials, to generate hybrid materials is an interesting strategy to improve scaffold mechanical properties, and degradation kinetics [83]. Synthetic polymers do not trigger immune reactions of the human body, and are also designed to modify the polymer material, in order to match the specific function of the biomaterial, without compromising its intrinsic properties. Among the most used synthetic polymers, there are: polycaprolactone, poly glycolic acid, and polyethylene glycol [84]. Natural polymers instead include collagen, hyaluronic acid, gelatin, alginate, chitosan, and silk fibroin [85]. Significant biocompatibility and biodegradability characterize this class of biomaterial; moreover, they are also considered as innate bioinformatic guidance for cells, able in promoting cell adhesion, stimulating the cellular chemotactic response, and regulating the biological interaction between scaffolds and tissues [86].

Because of their biodegradability, natural or synthetic polymer materials can promote cell adhesion, proliferation, and differentiation, with a wide range of promising applications in regenerative procedures.

CHAPTER 3 - AIM OF THE RESEARCH

Understanding the bio-morphological behavior of human cells, towards the biomaterials used for the regeneration procedures, is the key to successfully choosing and applying the appropriate biomaterials for specific clinical situations. Regenerative procedures applied several biomaterials for various techniques, such as sinus augmentation and periodontal defects. APCs are frequently used as biomaterial for the treatment for periodontal disease: this class of biomaterial contains a polymer of fibrin matrix and high concentration of growth factors. For these reasons, APCs showed considerable properties such as osteogenesis and osteoinduction and they are the elective choice for bone regeneration and the periodontal disease, due to their higher potential for regeneration. Anyway, limited availability, a second surgical site, and discomfort for the patients influence the application of these biomaterials. Thus, several classes of biomaterials have been proposed. The dentine is another material with an autologous nature, and recently considered a grafting material. Dentin is a mineralized tissue underneath the enamel, formed by 65% of inorganic material (HA) and 35% of organic material (collagen proteins and BMPs), elements which determined the biomaterial's osteoconductive and osteoinductive properties.

Furthermore, also xenografts are used for oral regeneration, specifically for periodontal, peri-implant and bone regeneration. Xenografts are characterized by significant osteoconductive properties and derived from bovine, porcine equine and marine origin. Among the most commonly used xenografts for regenerative purposes, there is the DBBM, whose regenerative properties relies from their physiochemical composition.

For these reasons, it appeared necessary to investigate the biological and morphological response of hPLFs exposed to these different classes of biomaterials, with the aim to evaluate their application in periodontal regeneration interventions.

CHAPTER 4 - MATERIALS AND METHODS

The application of the following materials and methods (Figure 2) provided biological and morphological evidence, published on Materials [59] and International Journal of Molecular Sciences [2,87]. According to the publisher (M.D.P.I.), ”the reuse of entire or part of the article, including figures and tables, does not require special permission. Any part of articles published under an open-access Creative Common CC BY license may be used without requiring permission, provided that the original article is clearly cited. The reuse of an article does not require MDPI and authors’ endorsement”.

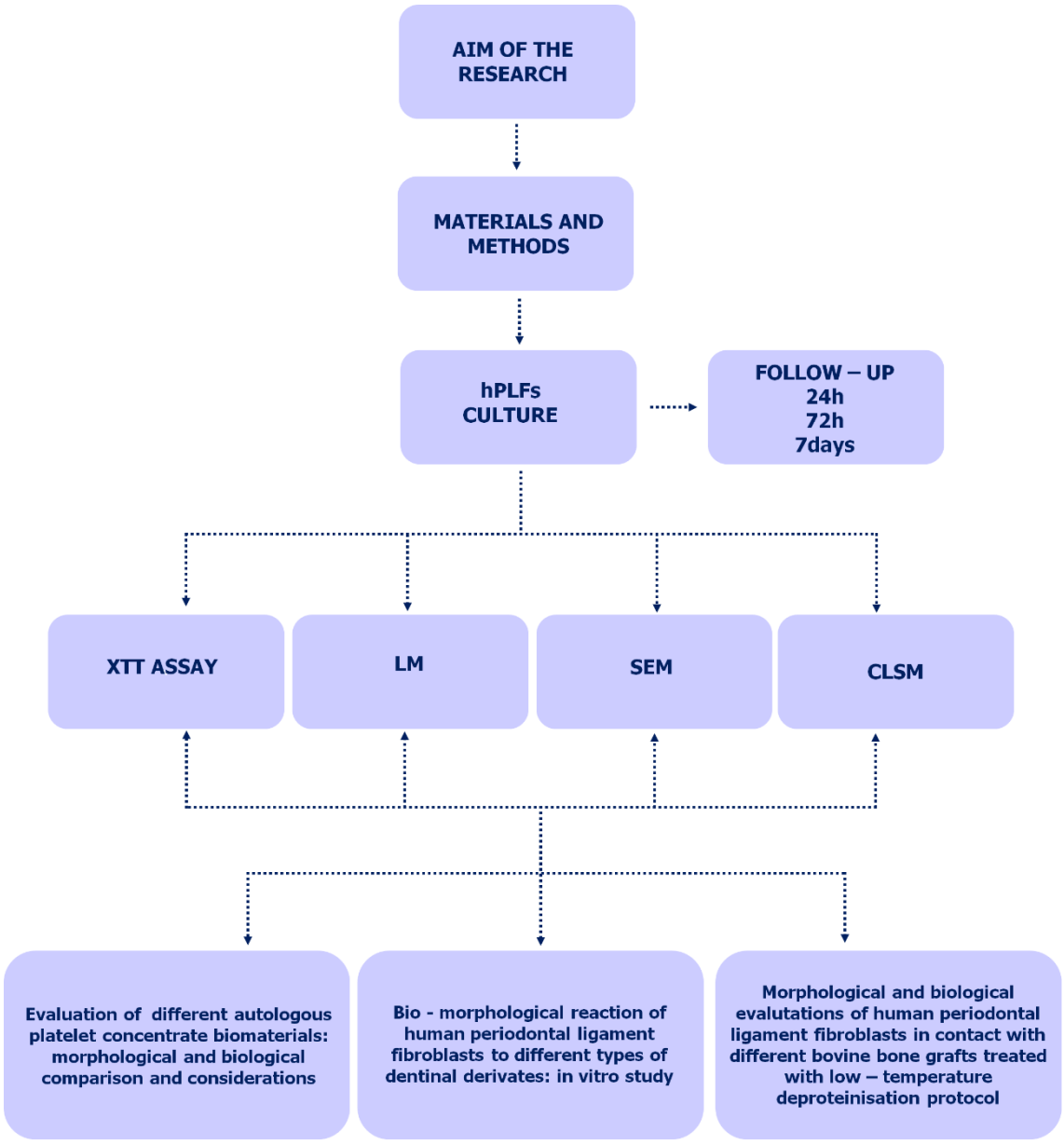

Figure 2. Study design and workflow of the research.

4.1 Evaluation of Different APCs: Morphological and Biological Comparisons and Considerations

4.1.1 Sampling Procedures and APC Preparation

"Blood samples were obtained from a healthy, 25-year-old, non-smoking Italian man. Furthermore, a written informed consent was provided, in accordance with the Helsinki Declaration on the Ethical Principles for Medical Research Involving Human Subjects [59]."

4.1.2 APC Preparation: L-PRF

"Twenty-seven millilitres (ml) of venous blood were collected in one dry glass tubes (9 mL in each) (Blood collecting tubes®, Process, Nice, France), without any anticoagulant. According to the standard Choukroun's protocol [56], tubes were immediately centrifuged at 2700 rpm (approximately 400× *g*) for 12 min with a dedicate centrifuge (Intra-lock International, Birmingham, AL, USA). In the middle of the tube, there was a fibrin dense clot, between the red cells at the bottom and the liquid serum called platelet-poor plasma at the top."

4.1.3 APC Preparation: CGF

"Sacco's protocol was used to obtain CGF [59] using a specific centrifuge (CGF, Silfradent, Santa Sofia, FC, Italy). According to this protocol, the centrifugation required acceleration for 30 s, 2700 rpm for 2 min, 2400 rpm for 4 min, 2700 rpm for 4 min, 3000 rpm for 3 min, deceleration for 36 s and then stopping."

4.1.4 APC Preparation: APG

"APG preparation included the collection of approximately 9 mL of blood into collection tubes. Subsequently, this sample was shaken to mix the anticoagulant with the blood. Tubes, containing sodium citrate 3.8%, were then centrifuged at 480 RCF for 4 min with a specific centrifuge (GF One, UBGEN, Padova, Italy). After this centrifugation, the blood sample was divided into different parts: a red-coloured fraction containing the red blood cells, a layer rich in platelets, a whitish layer containing white blood cells and the APG, consisting of the autologous fibrinogen.

According to this protocol, the layer rich in platelets was aspirated and APG was mixed with 10U of $CaCl_2$, to transform the liquid phase to gel phase. Time requested for this preparation, from venipuncture to injection, was approximately 10 min, and 1 mL of APG was produced per tube [59]."

4.1.5 Cell Culture

"HPLF cell line from ScienCell research Laboratories was cultured according to the manufacturer's instructions. Briefly, the initial vial containing 5×10^5 cells in 1 mL of volume was cultured in three plastic culture dishes in FM and incubated under standard cell culture conditions (37 °C in 5% CO_2). One bottle of FM is composed of the following: 500 mL of basal medium, 10 mL of FBS, 5 mL of FGS and 5 mL of penicillin/streptomycin solution (10,000 IU/mL of Penicillin, 10 μg/mL Streptomycin). When the cells reached sub-confluence, they were detached, by using 0.05% trypsin, and subcultured at a density of 110 cells/mm^2. For all experimental assays, subculture passages 7 or 8 were used [59]."

4.1.6 Cell Proliferation Assays and Statistical Analysis

"Cells were grown in 96 well plates, under standard cell culture conditions. Two micrograms of the tested material were plated into the 96 well microplates. After 24 h, 72 h and 7 days, the XTT Assay (Cayman Chemical, Ann Arbor, MI, USA) was used, to assess the proliferation activity of the cells, and the microplates were read at an absorbance wavelength of 450 nm. Proliferation of the negative control cultures was set at 100%. The XTT tests were performed with three technical replicates in three

independent experiments. The mean density of the test groups was divided by that of the control group and indicated as a percentage of the control value.

Two-way ANOVA was employed to analyse the grouped raw data, using GraphPad Prism 8.4.2 (GraphPad Software, San Diego, CA, USA), considering a p-value < 0.05 as significant [59].”

4.1.7 Morphological Analysis

“A qualitative evaluation of hPLFs was performed by LM, to have a first-sight overview of the culture, then through SEM and CLSM, with the aim to observe the eventual morphological changes [59].”

4.1.8 Morphological Analysis: LM

“Cells were plated in 30 mm diameter plastic culture dishes with the tested and the control material and incubated under cell culture conditions. After 24 h, 72 h and 7 days from the seeding, three dishes containing the tested material and other material were fixed using a 10% solution of formaldehyde and processed for light microscopy using Azan Mallory staining (Bio-Optica SpA, Milan, Italy), following the instructions of the manufacturer. Azan Mallory stain is used to process connective tissues and therefore indicated to stain

fibroblasts. Observations were performed through a light microscope (Zeiss, AxioImager A2, Jena, Germany) and photographed using a Leica DFC 320 digital camera (Leica DFC 320, Wetzlar, Germany) [59] ."

4.1.9 Morphological Analysis: SEM

"After 24 h, 72 h and 7 days from the seeding of the three dishes, containing cover glasses on which cell solutions, containing the tested material or the test control were seeded, cells were fixed using a 2% solution of glutaraldehyde and processed for SEM, as described previously [88]. Briefly, samples were dehydrated in ascending concentration ethanol solutions of 70%, 80%, 90% and three times 100%, for 10 min each. Subsequently, samples were immersed for 3 min in 100% HDMS (Sigma-Aldrich srl, Milan, Italy) and transferred into a desiccator, for 25 min to prevent water contamination. Afterwards, samples were air-dried by the evaporation of hexamethyldisilane (HDMS). Finally, samples were mounted on metal stubs, gold stained, and then observed by SEM (GEMINI_SEM, Zeiss, Germany) at different magnifications using secondary electrons and InLens probes [59]."

4.1.10 Morphological Analysis: CLSM

"Cells grown on a coverslip, in presence of the considered APCs for 24 h, 72h and 7 days were fixed with 4% PFA (Bio-Optica SpA, Milan, Italy) in PBS for 10 min, permeabilized with 0.1% Triton-X-100 for 5 min and incubated with a blocking solution (PBS containing 3% BSA), for 10 min at room temperature (RT). Subsequently, cells were incubated for 1h at RT, with the mouse monoclonal anti-CD90 (Thy-1)/fibroblast primary antibody [89] diluted in blocking solution (1:200, Chemicon International Inc. Temecula, CA, USA), and incubated with the donkey anti-mouse IgG Alexa Fluor 488 conjugated secondary antibody (1:2000, Immunological Science Rome, Roma, Italy) for 30 min at RT.

Cells were incubated with Phalloidin Alexa Fluor 546 diluted in blocking solution (1:100, Immunological Science Rome, Roma, Italy), for 30 min, at RT, to perform the actin staining. Finally, coverslips were mounted with Vectashield Mounting Medium with DAPI (Vector Laboratories, Burlingame, CA, USA) and examined with a Leica TCS SP5 confocal microscope (Mannheim, Germany). Regarding the controls, they were performed by omitting the primary antibody [59]."

4.2 Bio-Morphological Reaction of hPLFs to Different Types of Dentinal Derivates: In Vitro Study

4.2.1 Sampling Procedures and Dentine Derivates Preparation

"Four wisdom teeth were previously extracted due to surgical reasons. Samples were kindly provided from a healthy, 25-year-old, and non-smoking Italian woman, after obtaining her written informed consent, according to the Helsinki Declaration on the Ethical Principles for Medical Research Involving Human Subjects. Subsequently, teeth were stored in physiological solutions, used for dentine processing according to three different protocols:

- TT (Tooth Transformer S.r.l., Milan, Italy).
- Smart dentine Grinder (KometaBio Inc., Cresskill, NJ, USA), whose derived dentine will be named as SG.
- Smart dentine grinder within house protocol, whose derived dentine will be named as DDP.

Before starting the experimental procedures, all molars were cleaned from residual periodontal ligaments fibers and residual calculus, by using a piezoelectric instrumentation Piezon (EMS Electro Medical Systems SA, Nyon, Switzerland). All the

teeth were reduced into small pieces with a diamond torpedo bur # 0.12 (Komet Italia S.r.l., Milano, Italy), to facilitate mincing [87]."

4.2.2 TT Protocol

"The extracted tooth was completely processed in the mill with pre-calibrated blades and chemical solutions. After 25 five minutes of processing, dentine was ready to be used in cells culture. The particles size obtained, according to the manufacturer's instructions, is Ø < 1 mm [90]. The applied solutions were: (I) demineralization reagent, (II) and (III) washing solutions, (IV) sterilization reagent, and (V) and (VI) washing agents [87]."

4.2.3 The Smart Dentine Grinder Protocol

"This protocol consists of two solutions used after the milling process. Particles of Ø 0.25 to 1 mm were obtained. Chemical solutions applied are: (I) a dentine cleaner (0.5 mL Sodium Hydroxide with Ethanol) and (II) DPBS. After the milling process, particles were stored in a sterile container (mixing dish), and dentine cleanser was used to cover the entire particles for 5 min. After this first phase, the cleanser was removed, and the buffered solutions were added to clean the residues. This step, according to the manufacturer's instructions, was applied two times (Figure 3) [87]."

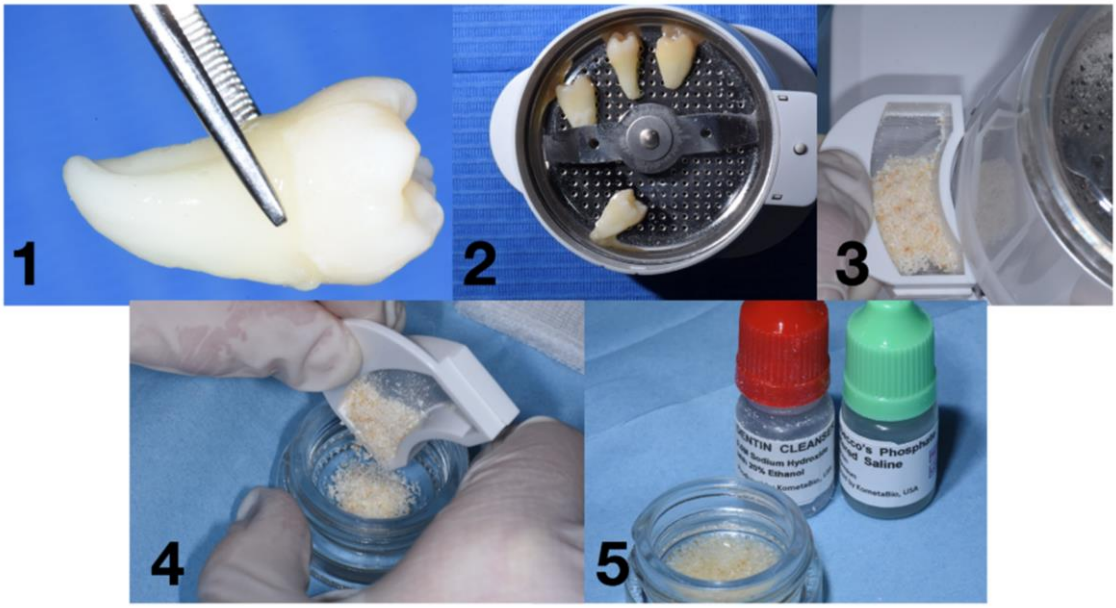

Figure 3. Workflow for the Smart Grinder protocol: *(1) Tartar and periodontal ligament removal, (2) milling process, (3) particles ready to be chemically treated, (4) particles in the mixing dish, and (5) particles after the chemical process [87].*

4.2.4 Smart Dentine Grinder Protocol Internally Modified

"Smart Dentine Grinder internally modified protocol consists of the replacement of the dentine detergent and demineralizer (0.5 mL sodium hydroxide with ethanol) with 0.5 mL of nitric acid 2% to demineralize the dentin. The conditioning time lasted 5 min [87]."

4.2.5 Control Material

"A demineralized and deproteinized bovine bone, commonly applied in dental surgical procedures (Geistlich Bio-Oss®, Granules 0.25–1 mm), was used as control material [87]."

4.2.6 Cell Culture

"HPLFs cell line from ScienCell Research Laboratories were cultured according to the manufacturer's instructions. The initial vial containing 5×10^5 cells in 1 mL of volume, was incubated under standard cell culture conditions (37 °C in 5% CO_2), and seeded in three plastic culture dishes with FM, characterized by the following composition: 500 mL of basal medium, 10 mL of FBS, 5 mL of FGS, and 5 mL of penicillin/streptomycin solution (10,000 IU/mL of Penicillin; 10 µg/mL Streptomycin). At a sub-confluence stage, the detachment stage followed using 0.05% trypsin, and subcultures with the density of 110 cells/mm^2 were initiated. The cells used for all experimental assays derived from eight subculture passages [87]."

4.2.7 Cell Proliferation Assays and Statistical Analysis

"Cells were incubated in 96 well plates under standard cell culture conditions. Two micrograms of the tested material were added to the 96 well microplates. At the moment of seeding (T0) and at 24 h (T1), 72 h (T2), and 7 days (T3) follow-up, XTT Assay (Cayman Chemical, Ann Arbor, MI, USA) was used to assess cellular proliferation activity, at a read absorbance wavelength of 450 nm. The XTT tests were performed with three technical replicates.

After assessing the normal distribution of the data, the two-way ANOVA test and Dunnett's post-hoc test for multiple comparisons were performed, to evaluate any significant variations within the experimental groups, considering the T0 and the T1, T2, and T3 follow-ups and between the experimental groups and the negative control at each follow-up. The Bonferroni post-hoc test was used to assess any significant variation between the experimental materials at each follow-up.

Statistical analysis and graphs were performed by using GraphPad Prism 9.1.1 (GraphPad Software, San Diego, CA, USA) [87]."

4.2.8 Morphological Analysis

"Qualitative evaluation of cells was performed by LM to have a first-sight overview of the culture. Then, SEM and CLSM were used to observe the eventual morphological reactions [87]."

4.2.9 Morphological Analysis: LM

"Cells were plated in 60 mm diameter plastic culture dishes, with tested and control material, and incubated under cell culture conditions. After 24 h, 72 h, and 7 days from the seeding, the dishes were observed by using a phase-contrast light microscope (ZEISS

Primovert, Jena, Germany) and a ZEISS Axiocam 208 color camera was used to capture the images at 10× and 20× [87].”

4.2.10 Morphological Analysis: SEM

“After 24 h, 72 h, and 7 days from the seeding of the 60 mm diameter plastic culture dishes containing the cover glasses the test (SG, DDP, and TT) and the control (BIOS) materials, cells were fixed by using a 2% solution of glutaraldehyde and processed for SEM, as previously described [91]. Briefly, the samples were processed for dehydration in ascending concentrations of ethanol solutions of 70%, 80%, and 90% and three times at 100% for 10 min each. Afterward, samples were immersed for 3 min in 100% HDMS (Sigma-Aldrich S.r.l., Milan, Italy). Subsequently, they were air-dried by the evaporation of HDMS and placed into a desiccator for 25 min to prevent water contamination. The samples were mounted on metal stubs, gold stained, and then observed by SEM (GEMINI_SEM, Zeiss, Germany) at different magnifications by using secondary electrons and InLens probes [87].”

4.2.11 Morphological Analysis: CLSM

"Cells seeded on coverslips were fixed with 4% PFA in PBS (10 min at RT), permeabilized with 0.1% Triton X-100 in PBS (5 min at RT), and the nonspecific binding sites were blocked with 10% BSA in PBS for 10 min at RT (blocking solution). After washing, cells were incubated with a mixture of mouse anti-Ki67 (Dako, Denmark A/S) and rabbit anti-vinculin (1:400, Immunological Sciences, distributed by Societa Italiana Chimici, Rome, Italy) primary antibodies (triple staining) or with mouse anti-Human integrin αVβ3 monoclonal antibody (single staining 1:300, Immunological Sciences) O/N at 4 °C. After the washings, primary antibodies were revealed by a mixture of Alexa Fluor 488 anti-mouse IgG and Alexa Fluor 633 anti-rabbit IgG secondary antibodies (1:2000) and Phalloidin Alexa Fluor 546 (1:300) (triple staining) or with Alexa Fluor 488 anti-mouse IgG secondary antibody alone (Immunological Sciences), for 30 min at RT. Furthermore, primary, and secondary antibodies were diluted in a blocking solution. The controls were performed by omitting the primary antibody. Coverslips were mounted with Vectashield Mounting Medium containing DAPI (Vector Laboratories, Burlingame, CA, USA) and observed at a Leica TCS SP5 confocal microscope (Leica, Mannheim,

Germany). Data were acquired by Leica LAS AF software, and a minimum of 20 images for each determination was analyzed [87].”

4.3 Morphological and Biological Evaluations of hPLFs in Contact with Different Bovine Bone Grafts Treated with Low-Temperature Deproteinisation Protocol

4.3.1 Biomaterials

"Deproteinised bovine bone grafts were harvested from young cattle (24 months), and after the first treatment of graft preparation for particle size and shape, a phase of purification through a thermic process was conducted. Grafts were subjected to a thermic shock, in the first phase at a high temperature (121 °C), and at a low temperature (80 °C; called Thermagen®) in the second phase.

The grafts (Figure 4) were divided into the following four experimental groups:

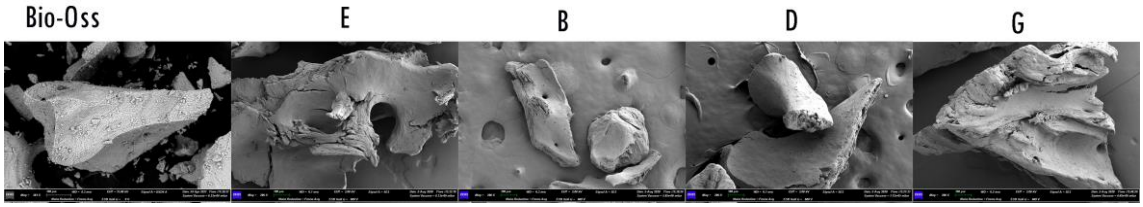

Figure 4. Scanning electron microscope (SEM) of bone grafts groups B, D, G, E, and Bio-Oss (BIOS). *According to the manufacturing instructions, the bone grafts groups B and D are mainly cortical, and the bone grafts group G appears more cancellous; magnification 200× [2].*

- **Group Bone E:** cancellous granules with a size between 0.25 and 1 mm, exposed to NaOH for 1 h for deproteinisation.

- **Group Bone B:** cortical and cancellous granules with a size between 0.25 and 1 mm, not exposed to NaOH for deproteinisation.
- **Group Bone D:** cortical and cancellous granules with a size between 0.25 and 1 mm, exposed to NaOH for 1 h for deproteinisation.
- **Group Bone G:** cancellous granules with a size between 1 and 2 mm, exposed to NaOH for 1 h for deproteinisation.

As a positive control, a graft of cancellous granules was designed with a size between 0.25 and 1 mm and exposed to NaOH for 1 h for deproteinisation at a high temperature (Bio-Oss, named BIOS in the experiment; Figure 4) [2]."

4.3.2 Cell Culture

"HPLFs were used and cultured as suggested by the manufacturer's instructions (ScienceCell Research Laboratories, Carlsbad, CA, USA). Initially, the first vial containing 5×10^5 cells in 1 mL of volume was cultured in four plastic culture dishes in FM (Innoprot. Derio, Bizkaia, Spain). Dishes were incubated under standard cell culture conditions (37 °C in 5% CO_2). FM was composed of a 500 mL basal medium, 2% FBS, 1% FGS, and 1% penicillin–streptomycin solution. At subconfluence stage, cells were detached using 0.05% trypsin (Innoprot. Derio, Bizkaia, Spain) and then subcultured at a

density of 110 cells/mm^2. Thus, the subculture passage used for the experimental phase was 10. HPLF is a cellular line characterized by the production of osteoblast-related extracellular matrix proteins, alkaline phosphatase activity, and active participation in inflammatory and immune-related events during periodontal diseases [92,93]. The hPLFs model was applied to evaluate the behavior of periodontal cells in cases of use of xenografts in periodontal defects regeneration, by virtue of the mentioned properties [2]."

4.3.3 Cell Proliferation Assay and Statistical Analysis

"The cell proliferation assay was performed according to the ISO EN 10993-5 standard. Briefly, 1 g of each sterile sample was placed into 24-well plates. Then, 1 mL of FM was added (extraction medium) to each well and incubated for 24 h at 37 °C. Under standard cell culture conditions, 10^3 cells per well were seeded in a 100 µL extracted DMEM medium. The negative control group was seeded in FM. XTT assay (Cayman Chemical, Ann Arbor, MI, USA) allowed observation of the cellular starting condition (T0) and proliferation activity at 24 h (T1), 72 h (T2), and 7 days (T3) follow-ups at an absorbance wavelength of 450 nm. XTT tests were performed with three technical replicates.

After assessing the normal distribution of the data, a two-way analysis of variance (ANOVA) test and Dunnett's and Bonferroni's post hoc analyses for multiple

comparisons were performed to evaluate any significant variation between T0 and T1, T2, and T3 follow-ups.

GraphPad Prism 9.1.1 (GraphPad Software, San Diego, CA, USA) was used to perform statistical analysis and graphs [2].”

4.3.4 Morphological Analysis

“A morphological evaluation of cells was performed using LM to obtain a first-sight overview of the shape of the cultured cell. SEM was used to observe the cell membrane reaction, and CLSM was used to assess morphological changes in the cytoskeleton [2].”

4.3.5 Morphological Analysis: LM

“Cells were seeded in 60 mm diameter plastic culture dishes with the test materials, control material, and without the material and then incubated under cell culture conditions. At T1, T2, and T3 follow-ups, dishes were observed using a phase-contrast light microscope (ZEISS Primovert, Jena, Germany), and a ZEISS Axiocam 208 colour camera was used to capture the images at 10× and 20× [2].”

4.3.6 Morphological Analysis: SEM

"At T1, T2, and T3 follow-ups the cells, seeded on a covered glass in 60 mm diameter plastic culture dishes containing the test materials or the control, were fixed using a 2% solution of glutaraldehyde, dehydrated in an ascending concentration ethanol solutions scale of 70, 80, and 90%, and three times at 100% for 10 min each. Afterwards, samples were immersed for 3 min in 100% HDMS (Sigma-Aldrich S.r.l., Milan, Italy). Afterwards, the samples were air-dried by evaporation of HDMS. After transferring the sample into a desiccator to prevent water contamination, the covered glasses were mounted on metal stubs, gold stained, and then observed using SEM (GEMINI_SEM, Zeiss, Germany), at different magnifications, using secondary electron probes [2]."

4.3.7 Morphological Analysis: CLSM

"HPLFs grown on coverslips in presence or absence of test materials for T1, T2, and T3 follow-ups were fixed with 4% PFA in PBS for 10 minutes at RT. Then, hPLFs were permeabilised with 0.1% Triton X-100 in PBS for 5 minutes at RT. After washing, the nonspecific binding sites were blocked with 3% BSA in PBS (blocking solution) for 10 min at RT. For double immunostaining, cells were incubated with mouse monoclonal anti-CD90 (Thy-1)/fibroblast primary antibody (Chemicon International Inc., Temecula,

CA, USA), diluted 1:200 in blocking solution, O/N at 4 °C. After washings, cells were incubated with a mixture of Alexa Fluor 488 anti-mouse IgG secondary antibody (1:2000) and Phalloidin Alexa Fluor 546 (1:300; Immunological Science, distributed by Società Italiana Chimici, Rome, Italy) in blocking solution for 30 min at RT. Internal controls of the fluorescence and functionality methodology were performed, by omitting the primary antibody. Coverslips were mounted with Vectashield Mounting Medium containing DAPI (Vector Laboratories, Burlingame, CA, USA) and observed by a Leica TCS SP5 confocal microscope (Leica, Mannheim, Germany). Data for actin morphology assessment were acquired using Leica LAS AF software, and a minimum of 20 images for each determination were analyzed [2].”

CHAPTER 5 - RESULTS

The results of the following studies contributed to three different manuscripts published on Materials [57] and International Journal of Molecular Sciences [2,87]. According to the publisher (M.D.P.I.), ”the reuse of entire or part of the article, including figures and tables, does not require special permission. Any part of articles published under an open-access Creative Common CC BY license may be used without requiring permission, provided that the original article is clearly cited. The reuse of an article does not require MDPI and authors’ endorsement”.

5.1 Evaluation of Different APCs: Morphological and Biological Comparisons and Considerations

“XTT analyses and morphological observations provided an integrated overview of the performance of the examined biomaterials in contact with the hPLFs [59].”

5.1.1 Cell Proliferation Assays and Statistical Analysis

“Data derived from cell proliferation assays showed that cells exposed to L-PRF and CGF increased their proliferation at all the considered times concerning control with 100% viability (Figure 5). Specifically, the CGF condition showed better performance at 24 and

72 h, characterized by 146% and 166% values, respectively, while the L-PRF displayed 125% and 145% proliferation values at 24 and 72 h, respectively. Moreover, APG showed a low level of proliferation, characterized by a value of 128% during the first 72 h. CGF showed the highest hPLFs cell proliferation at 7 days [59]."

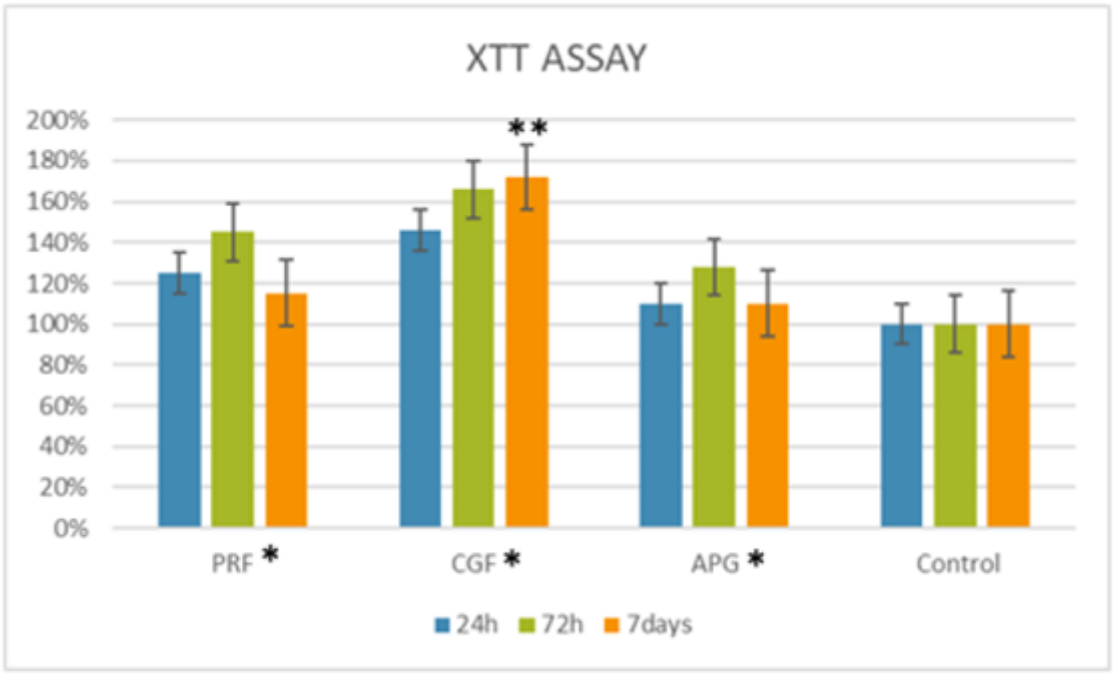

Figure 5. XTT assay of hPLFs cells in contact with the APCs at different times. *For 24 h, PRF displayed the highest peak, followed by the CGF and APG. CGF performed best at 72h and 7 days, followed by the PRF and APG. The biomaterial proliferation values were statistically significant (*) with a p-value < 0.05 compared to the control, as suggested by the two-way ANOVA. Furthermore, the mean of the proliferation with CGF compared to control was statistically significant at 7 days (**), as highlighted by Dunnett's multiple comparison tests [59].*

"As shown in Figure 5, the two-way ANOVA analysis highlighted a statistical difference for the "biomaterials" parameter. The multiple comparison tests performed among the considered materials highlighted a statistically significant difference for the CGF at 7 days at the examined times [59]."

5.1.2 Morphological Analysis: LM

"LM analysis unveiled the presence of a uniform layer of healthy cells in all groups, characterized by differences between them (Figure 6) [59]."

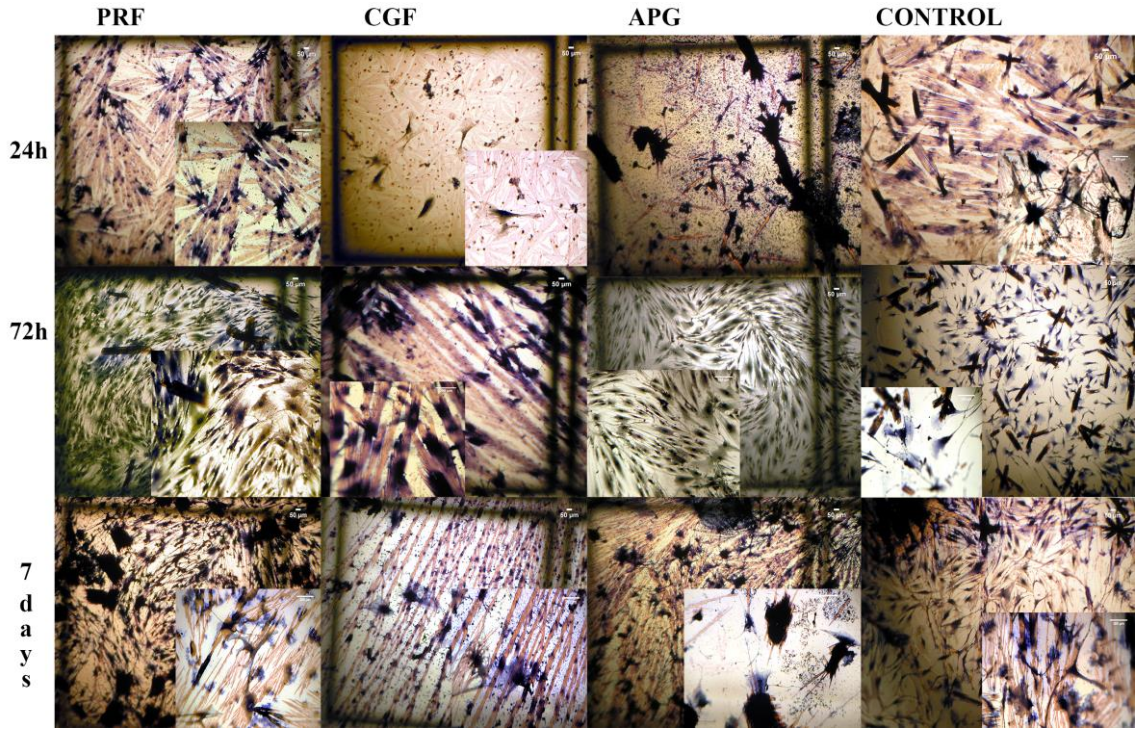

Figure 6. LM images of hPLFs with APCs and the controls at the different examined times. *The observed brown particles are PBS salts. Azan Mallory staining. Magnification, 4×. Insets' magnification: 10× [59].*

The control group showed densely packed cells, characterized by a fusiform morphology and small dimensions, at 24 h of culture. Instead, all experimental groups displayed slightly larger cells distant from each other. In CGF and APG groups, there are sporadic polygonal cells with cytoplasmatic extensions [59]."

“At 72 h, there was an overlapping of L-PRF cells with the homologous 24 h ones. Besides, CGF and APG showed more polygonal cells with a composite network of cytoplasmic processes. At 7 days, the control group displayed fusiform cells, while fibroblast cultured in the CGF and L-PRF groups appeared large and polygonal. By this point, the APG group also showed few fusiform cells [59].”

5.1.3 Morphological Analysis: SEM

"SEM observations revealed that all experimental groups showed abundant, flattened, healthy cells (Figure 7) [59]."

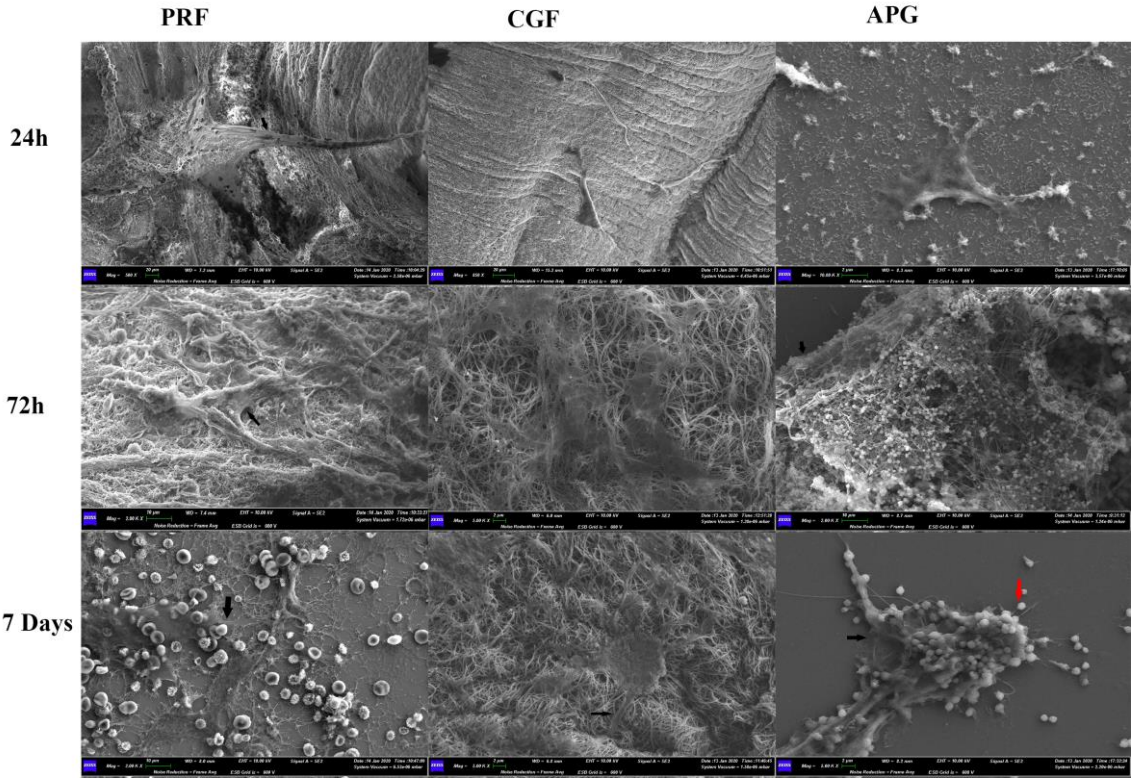

Figure 7. Representative SEM images of hPLFs and APC showing the morphological reaction of the hPLFs to the fibrin network, assuming a polygonal shape. *The three APCs displayed evident morphological differences in the fibrin networks, with blood cells with PRF and platelets with APG. Cellular projections toward the biomaterials were observed (black arrows). Moreover, platelets in the APG were also detected (red arrow). A morphological reaction of fibroblasts trying to envelop the platelets was detected in the APG samples [59].*

"After 24 h of culture, polygonal and elongated cells were detectable, with thick cytoplasmic digitations attributable to developing lamellipodia."

In the 72 h groups, cells were larger and anchored to APCs through numerous cell contacts. The latter included thin cytoplasmic digitations, such as filopodia, and larger

digitations, such as lamellipodia. After 7 days of culture, cells exhibited an extensive network of intercellular contacts. Filopodia and lamellipodia were abundant, and the intimate relationship between cell digitations and the APC elements was observed at higher magnification micrographs [59].”

5.1.4 Morphological Analysis: CLSM

“CLSM analyses investigated the status of the nuclei (blue) and the distribution of the actin (red). Oval or rounded (blue) nuclei were well represented in all samples, while actin staining differed between the groups. The control group showed a weak red signal; only after 7 days of culture a slight increase was noticeable. Generally, a progressive intensification of the red signal occurred during the culture period, in all APC samples (Figure 8) [59].”

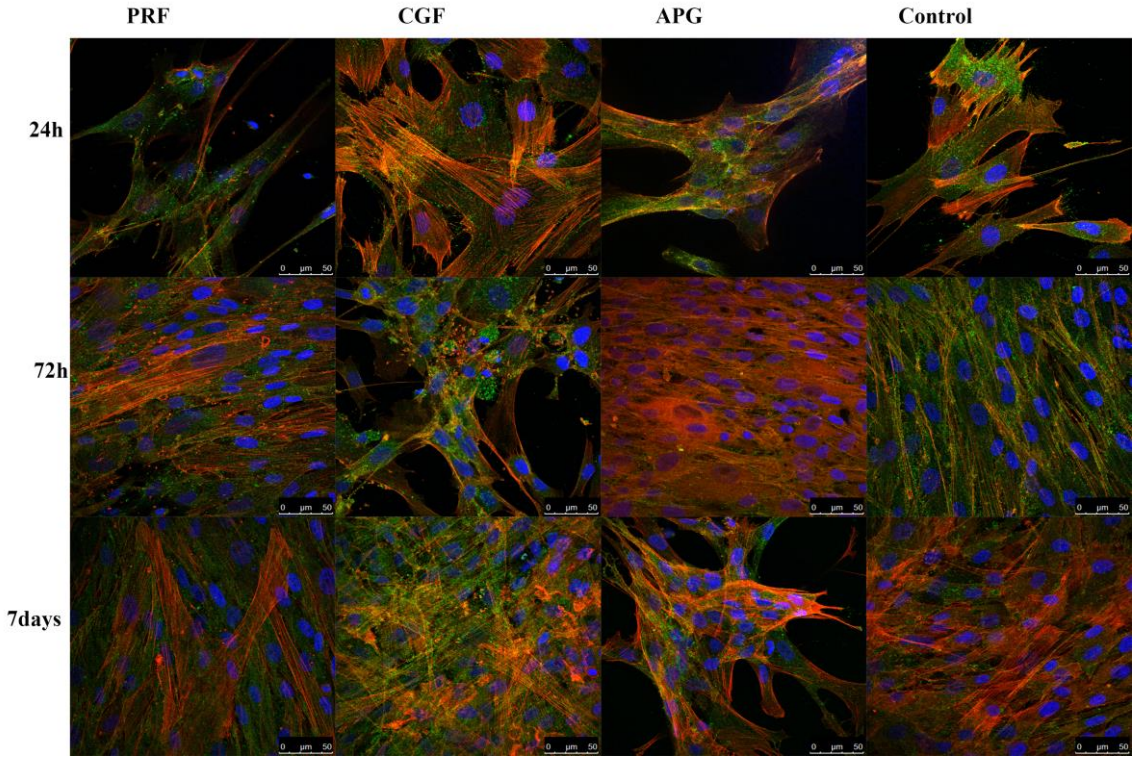

Figure 8. CLSM images of actin filaments revealed by phalloidin in control and treated hPLF at different times, including the hPLF under the three considered conditions and the controls at different times. *Low magnification. CD90, used as an hPLF marker, is green-stained. Actin is intensively represented compared to the control. Fibroblasts exposed to PRF displayed an intense actin stain inside the cellular projections, already at 72 h and more so at 7 days. HPLFs in contact with CGF showed a heavily modified and solicited actin. Furthermore, APG showed an intense representation of the actin fibers at 72 h [59].*

"Higher magnifications (Figure 9) investigated the detailed intracellular and intercellular distribution of actin. The control group detected it mainly in short projections, which remained close to the cellular body (*green—CD90*) and beneath the plasma membrane. On Day 7, despite an increase in the red signal, cells appeared densely packed, and no overlapping of projections was visible. In APCs, cytoplasmic projections formed bundles parallel to the major axis of the cellular extensions, and samples were characterized by strong red signals. Projections passed on neighboring cells and overlapped each other,

creating a rich three-dimensional network between different cells. The nuclei were distant in CGF and PRF, especially after 72h and 7 days. Besides the definite cellular protrusions, the space between the cell bodies was filled with large cytoplasmic extensions, displaying the delicate and uniform red signal. APG nuclei were closer, with a dynamic almost similar to the control ones [59]."

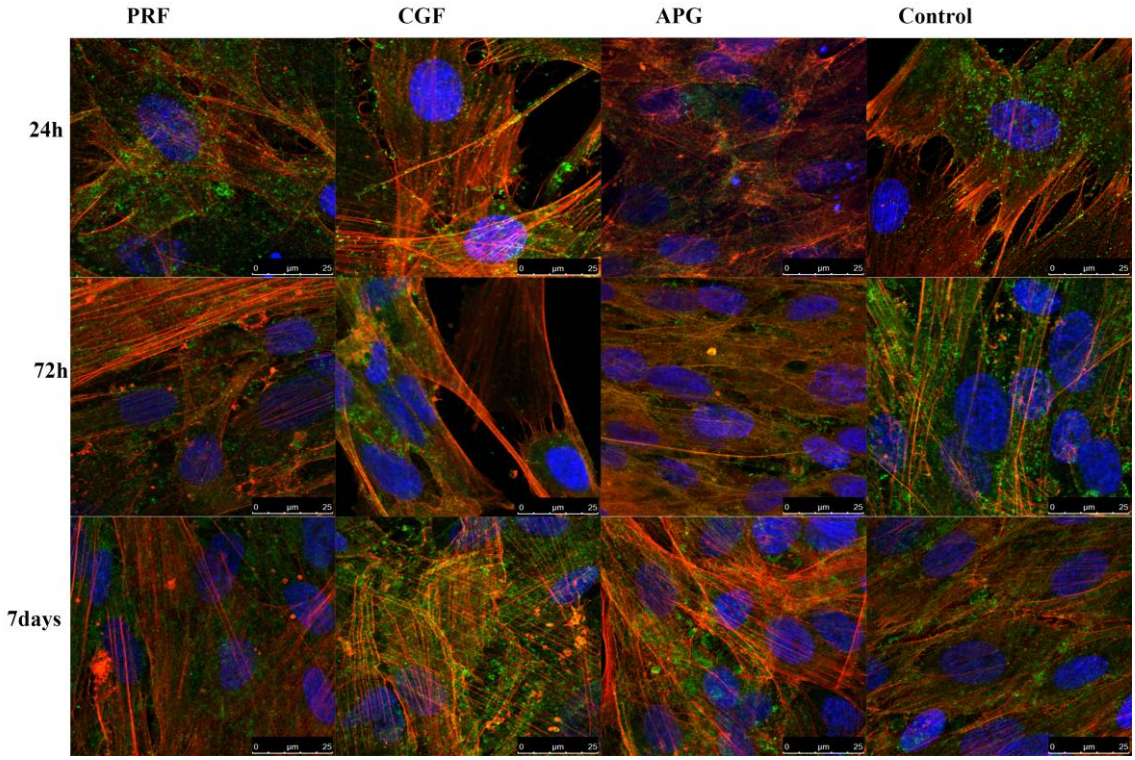

Figure 9. CLSM representative images, at a higher magnification, of actin filaments in treated hPLF and control. *In CGF 72 h observations, large cytoplasmic extensions filled the spaces between the cells, displaying a delicate and uniform red signal [59].*

5.2 Bio-Morphological Reaction of hPLFs to Different Types of Dentinal Derivates: In Vitro Study

5.2.1 Cell Proliferation Assays and Statistical Analysis

"The proliferation assays showed a proliferation growth curve (Figure 10) in tested dentinal grafts (SG, DDP, and TT), positive control material (BIOS), and negative control (no material) [87]."

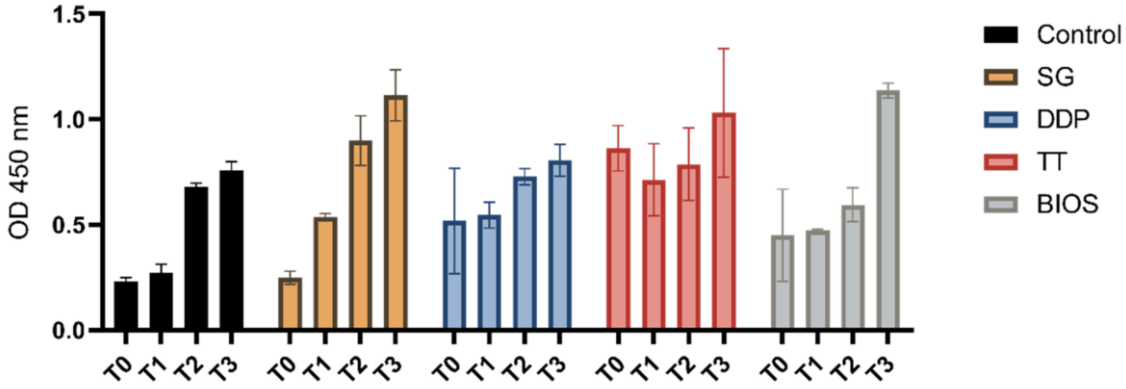

Figure 10. Mean and SD data of the optical density values (Y-axis) of the control (hPLFs not exposed to dentinal derivates), the cells exposed to tested materials (SG, DDP, and TT), and the cells exposed to the positive control material (BIOS) at the different timings (T0 - moment of seeding; T1 - 24 h after seeding; T2 - 72 h after seeding; and T3 - 7 days after seeding) **[87].**

"The two-way ANOVA tests were statistically significant, analyzing the variation of the OD from the moment of seeding (T0) and the other follow-up (T1, T2, and T3). Post-hoc Dunnett's analysis showed a significant variation of the growth in T2 and T3 follow-up in the negative control. There was a significant variation in positive control BIOS and the DDP experimental group at the T3 follow-up [87]."

"SG experimental group showed a significant variation at the T1, T2, and T3, while TT experimental group displayed a statistically significant variation between T0 and T1, T2, and T3 (Table 1) [87]."

Two-Way ANOVA Comparison the Different Time of Follow-Up			
Source of Variation	**% of Total Variation**	**F (DFn [1]; DFd [2])**	***p* Value**
Interaction	17.19	F (12.40) = 4.149″	0.0003
Time	51.85	F (3 40) = 50.04″	<0.0001
Treatment	17.14	F (4.40) = 12.40″	<0.0001
Dunnett's Analysis	**Mean Diff.**	**95.00% CI of diff.**	***p* Value**
Control			
T0 vs. T1	−0.040	−0.29 to 0.21	ns
T0 vs. T2	−0.44	−0.70 to −0.19	0.0003
T0 vs. T3	−0.52	−0.77 to −0.27	<0.0001
SG			
T0 vs. T1	−0.28	−0.54 to −0.03	0.02
T0 vs. T2	−0.65	−0.90 to −0.39	<0.0001
T0 vs. T3	−0.86	−1.12 to −0.61	<0.0001
DDP			
T0 vs. T1	−0.02	−0.28 to 0.22	ns
T0 vs. T2	−0.21	−0.46 to 0.04	ns
T0 vs. T3	−0.28	−0.54 to −0.03	0.02
TT			
T0 vs. T1	0.14	−0.06 to 0.36	ns
T0 vs. T2	0.07	−0.13 to 0.28	ns
T0 vs. T3	−0.16	−0.37 to 0.04	ns
BIOS			
T0 vs. T1	−0.02	−0.23 to 0.18	ns
T0 vs. T2	−0.14	−0.35 to 0.06	ns
T0 vs. T3	−0.68	−0.89 to −0.47	<0.0001

[1] Number of degrees of freedom; [2] degrees of freedom error.

Table 1. Summary of the two-way ANOVA comparison and Dunnett's multiple comparison test considering the time factor [87].

Table 1. Summary of the two-way ANOVA comparison and Dunnett's multiple comparison test considering the time factor [87].

"The two-way ANOVA tests, considering the variation of the OD between the experimental groups and the negative control at the moment of seeding (T0) (to assess any difference absorbance differences of the considered materials) and the other follow-ups (T1, T2, and T3) were statistically significant. The post-hoc Dunnett's analysis showed a significant variation of the growth at the T1 follow-up between the negative control group and experiment groups TT and DDP and a significant growth variation at the T3 follow-up between the negative control group, and the experimental groups' SG, TT, and BIOS (Table 2) [87]."

Two-Way ANOVA Comparison the Different Time of Follow-Up			
Source of Variation	**% of Total Variation**	**F (DFn [1]; DFd [2])**	***p* Value**
Interaction	17.19	F (12.40) = 4.149″	0.0003
Time	51.85	F (3.40) = 50.04″	<0.0001
Treatment	17.14	F (4.40) = 12.40″	<0.0001
Dunnett's Analysis	**Mean Diff.**	**95.00% CI of diff.**	***p* Value**
T0			
Control vs. SG	−0.01	−0.28 to 0.24	ns
Control vs. DDP	−0.28	−0.55 to −0.02	0.03
Control vs. TT	−0.63	−0.89 to −0.36	<0.0001
Control vs. BIOS	−0.21	−0.48 to 0.04	Ns
T1			
Control vs. SG	−0.26	−0.52 to 0.00	ns
Control vs. DDP	−0.27	−0.53 to −0.00	0.04
Control vs. TT	−0.44	−0.70 to −0.17	0.0005
Control vs. BIOS	−0.20	−0.46 to 0.06	ns
T2			
Control vs. SG	−0.22	−0.48 to 0.04	ns
Control vs. DDP	−0.04	−0.31 to 0.21	ns
Control vs. TT	−0.10	−0.37 to 0.15	ns
Control vs. BIOS	0.08	−0.18 to 0.34	ns
T3			
Control vs. SG	−0.35	−0.62 to −0.09	0.0053
Control vs. DDP	−0.04	−0.31 to 0.21	ns
Control vs. TT	−0.27	−0.53 to −0.00	0.04
Control vs. BIOS	−0.37	−0.64 to −0.11	0.002

[1] Number of degrees of freedom; [2] Degrees of freedom error.

Table 2. Summary of the two-way ANOVA comparison and Dunnett's multiple comparison test considering the exposure to the different materials [87].

"The post-hoc Bonferroni analysis showed a significant variation in the T3 follow-up between the DDP and BIOS groups (Table 3) [87]."

Bonferroni Analysis	Mean Diff.	95.00% CI of Diff.	*p* Value
T1			
SG vs. DDP	−0.01	−0.33 to 0.31	ns
SG vs. TT	−0.17	−0.50 to 0.14	ns
SG vs. BIOS	0.06	−0.26 to 0.38	ns
DDP vs. TT	−0.16	−0.49 to 0.15	ns
DDP vs. BIOS	0.07	−0.25 to 0.39	ns
TT vs. BIOS	0.24	−0.08 to 0.56	ns
T2			
SG vs. DDP	0.17	−0.15 to 0.49	ns
SG vs. TT	0.11	−0.21 to 0.43	ns
SG vs. BIOS	0.30	−0.02 to 0.63	ns
DDP vs. TT	−0.05	−0.38 to 0.26	ns
DDP vs. BIOS	0.13	−0.19 to 0.45	ns
TT vs. BIOS	0.19	−0.13 to 0.51	ns
T3			
SG vs. DDP	0.30	−0.01 to 0.63	ns
SG vs. TT	0.08	−0.24 to 0.40	ns
SG vs. BIOS	−0.02	−0.34 to 0.30	ns
DDP vs. TT	−0.22	−0.55 to 0.10	ns
DDP vs. BIOS	−0.33	−0.65 to −0.00	0.04
TT vs. BIOS	−0.10	−0.43 to 0.22	ns

Table 3. Bonferroni multiple comparison test considering the exposition to the different materials [87].

5.2.2 Morphological Analysis: LM

"LM analysis showed a layer of healthy fibroblasts, in the cells exposed to the dentinal materials and the bone material used as control, with morphological differences between them (Figure 11). At 24 h of culture, cells exposed to DDP and TT dentinal material appeared larger and with a polygonal shape; moreover, cells exposed to the SG and positive control BIOS were large but presented a more fusiform shape when compared with DDP and TT groups. All the cells presented cytoplasmatic extensions in the proximity of the biomaterial. At 72 h, cultured hPLFs appeared to be of higher density. In all samples, the cells' shape was large and polygonal, with a high presence of

cytoplasmatic processes, in the proximity of the material. Cells of the TT group presented small white particles inside the body. At 7 days, the cells of the DDP group continued to present a large and polygonal shape, as well as the cells of the TT group, which also continued to present small white particles inside the body. Fibroblasts of SG and BIOS appeared polygonal with a more fusiform morphology [87].”

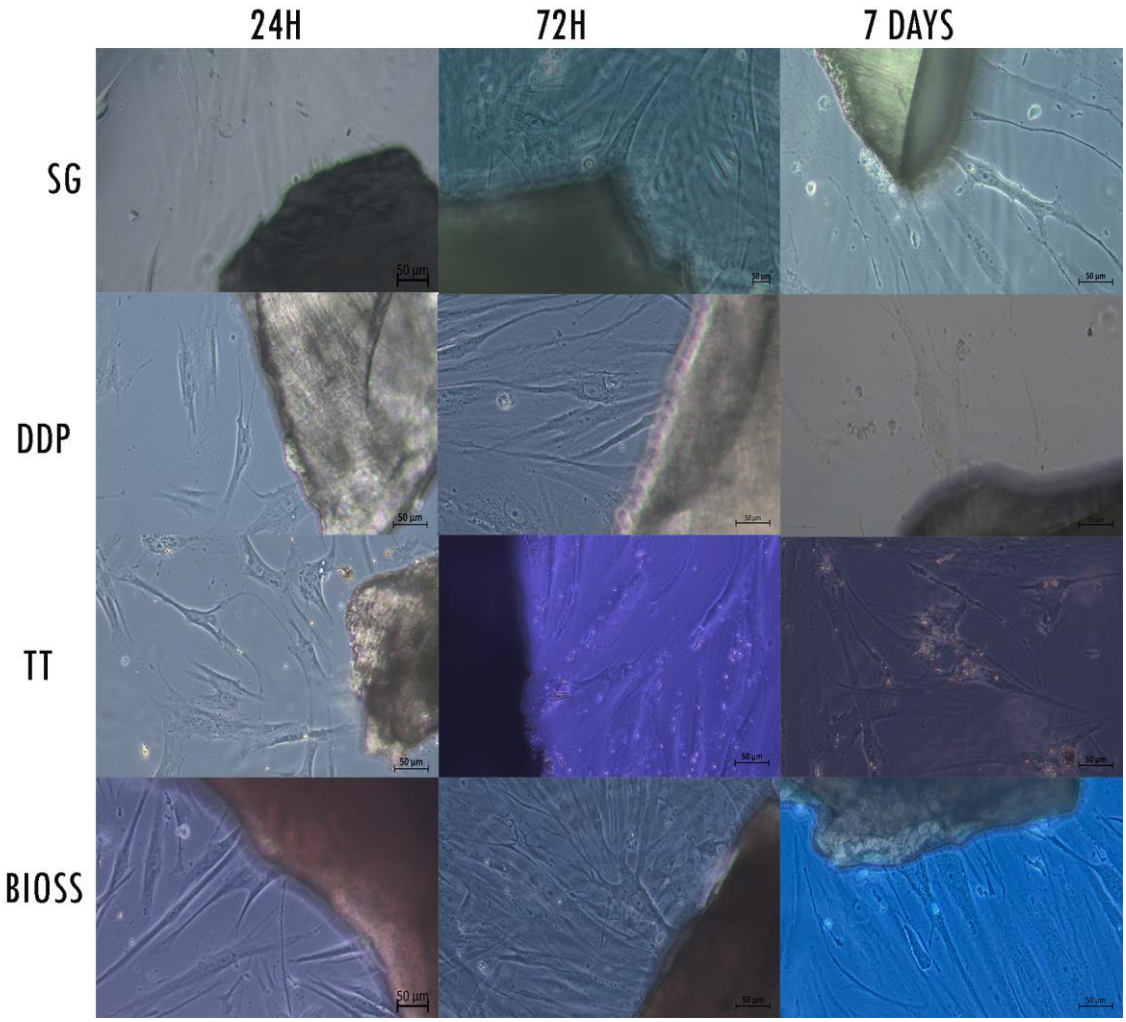

Figure 11. LM images of hPLFs with the examined materials and the negative control at 24h, 72h and 7 days. *Magnification 20×[87].*

5.2.3 Morphological Analysis: SEM

"SEM observation of the raw material highlighted morphological differences between the tested dentinal materials and positive control (Figure 12). Specifically, the peculiar morphology of the dentinal materials was appreciable. The external morphology of SG and DDP was overlapping, with the presence of the dentinal tubules. Since DDP was submitted to the demineralization protocol, the surface appeared smoother than the SG. The morphology of the TT sample appeared more irregular and jagged; the machine ground the dentin, and it was possible to observe the internal portion of the tubules. BIOS sample appeared with an irregular surface of mineralized bone [87]."

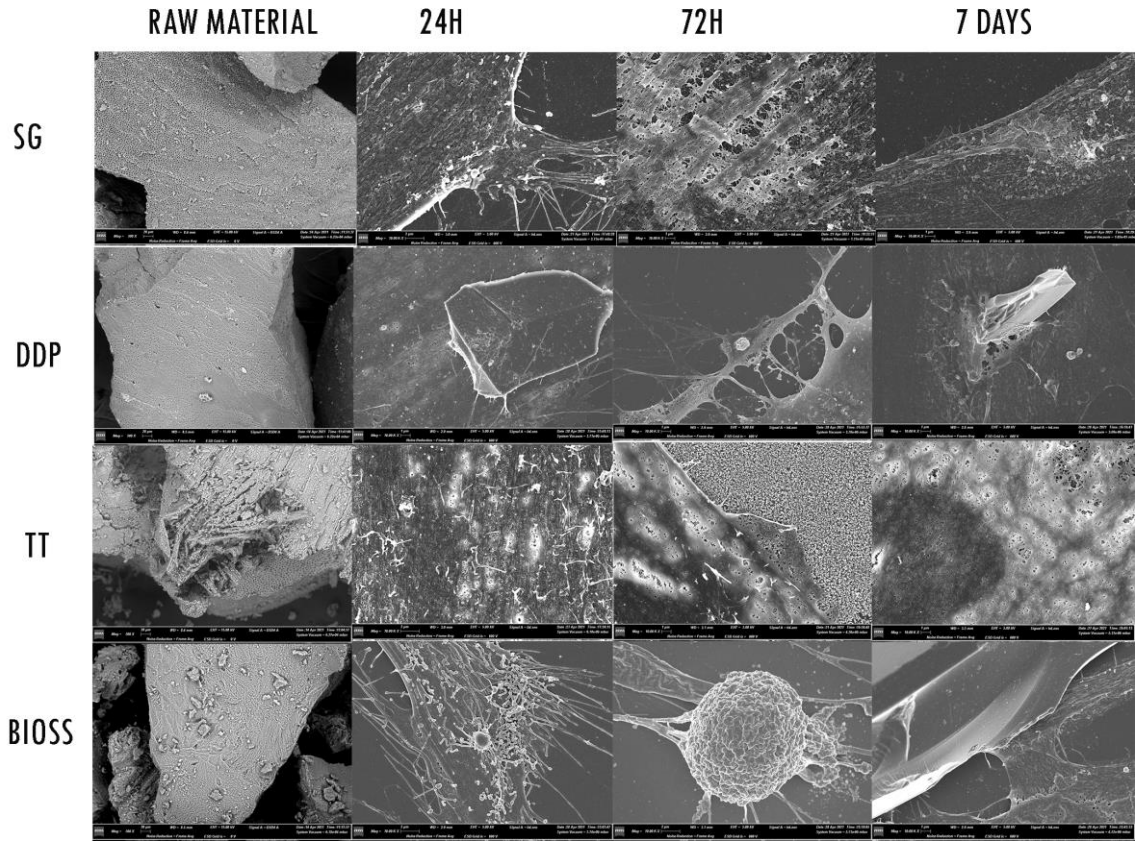

Figure 12. SEM images. *The first column on the right shows the SEM of the different Raw Materials. Magnification 200×. The other columns show the different reactions of the fibroblasts when exposed to the experimental materials SG, DDP, and TT and the positive control BIOS at 24 h, 72 h, and 7 days. Magnification 1000× [87].*

"Regarding fibroblasts' behavior at 24h, the cells body, exposed to the experimental biomaterials (SG, DDP, and TT), appeared enlarged and had cytoplasmatic extensions. The surface of cells exposed to SG and TT also presented digitation on the membrane. HPLFs in contact with DDP were flat, covering the biomaterial but without an external cellular reaction. Cells in contact with positive control BIOS presented different cytoplasmatic extensions on the membrane's surface. At 72 h, different reactions of the cells exposed to experimental biomaterials were observed. HPLFs in contact with SG and

BIOS presented thicker membrane surface, with cytoplasmatic eversions, while HPLFs exposed to DDP and TT showed flat membrane, with cytoplasmatic projections toward the biomaterials. The surface of the cells exposed to TT showed tiny holes. At 7 days, the surface morphology of the cells exposed to SG and BIOS materials continued to appear highly dynamic, with progressive thickening and cytoplasmatic digitations attributable to lamellipodia and filopodia. The morphology of the surface of HPLFs in contact with DDP and TT continues to be flattened and characterized by cytoplasmatic extension toward the biomaterials. The membrane surface of fibroblasts exposed to TT continues to present tiny holes [87]."

5.2.4 Morphological Analysis: CLSM

"CLSM observations evaluate the status of the nuclei, the expression of cytoskeleton elements, such as actin, vinculin, and integrins, and the proliferative state of the cells (Figure 13). Oval or rounded (blue) shaped nuclei were well-represented in all samples. The proliferation marker was present in all samples and all follow-ups [87]."

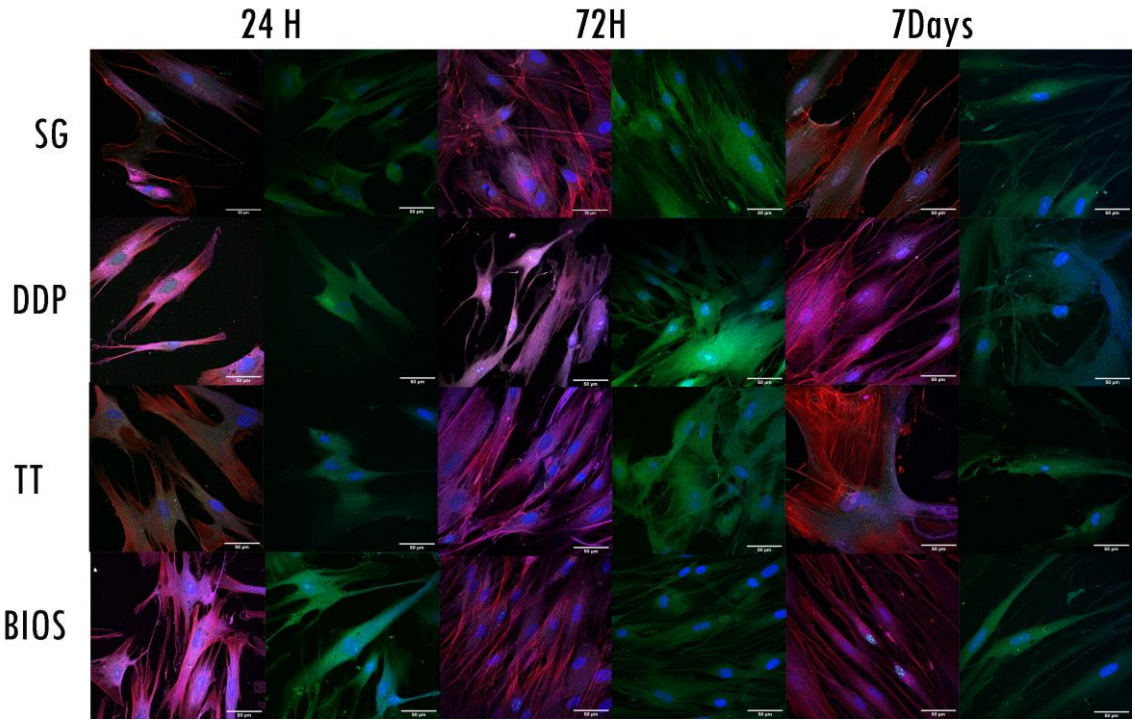

Figure 13. CLSM images. Each row represents the exposure of the fibroblast to the different biomaterials. *For each follow-up, two columns with different fluorescence stains are shown: The first one from the left shows the expression of proliferation (green signal-anti-Ki67) and the expression of actin filaments (red signal-phalloidin), vinculin (magenta signal- vinculin), and the nuclei (blue signal-DAPI). The second stain shows integrin expression (green signal-integrin αVβ3). Nuclei are stained with DAPI (blue signal). Magnification at 63× [87].*

"Regarding the expressions of the cytoskeletal markers, HPLFs in contact with SG expressed vinculin, integrin, and actin in all the follow-ups. Vinculin and integrin signals were stronger at 72 h, while the actin signal remained constantly expressed in all the

follow-ups and well distributed in the cytoplasmatic projections. HPLFs exposed to DDP expressed vinculin, integrin, and actin in all the follow-ups. The integrin signal was stronger at 72 h. At 7 days follow-up, stronger vinculin and actin signals were reported. The actin filaments were distributed into cytoplasmatic projections [87]."

"Furthermore, fibroblasts exposed to TT material expressed vinculin, integrin, and actin in all the follow-ups. The actin signal was stronger at 24 h and 7 days follow-ups, distributed in the cellular projections and cellular body. The stronger vinculin and integrin signals were reported at 72 h follow-up. HPLFs in contact with BIOS expressed vinculin, integrin, and actin in all the follow-ups. At 24 h follow-up stronger vinculin and integrin signals were reported. Actin signal was stronger at 72 h and 7 days follow-ups, distributed along with the cytoplasmatic projections [87]."

5.3 Morphological and Biological Evaluations of hPLFs in Contact with Different Bovine Bone Grafts Treated with Low-Temperature Deproteinisation Protocol

5.3.1 Proliferation Assay

"The examined materials (E, B, D, G), positive control (BIOS), and negative control (no material) displayed growth in the proliferation curve, as suggested by proliferation assays (Figure 14). The two-way ANOVA was statistically significant ($p < 0.05$), evaluating the variation in the OD from the T0 and T1, T2, and T3 follow-ups. A significant variation in the growth curve was observed in negative control and all the experimental materials from the T0 but also in groups exposed to experimental group E and BIOS at the T1 follow-up (Table 4), as highlighted by post hoc Dunnett's analysis. Instead, at any follow-up, no significant variations in the growth curve were detected by the post hoc Bonferroni analysis [2]."

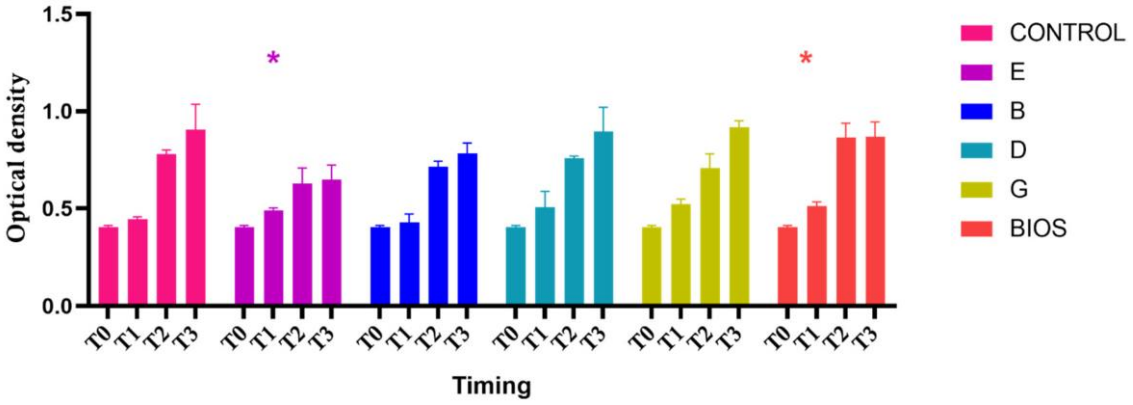

Figure 14. Mean and SD grouped data of the optical density values (Y-axis) of the hPLFs not exposed to materials (control) and exposed to the different bovine bone grafts (B, D, G, E, and BIOS) at different examined times (T0, T1, T2, and T3). ** Indicates the two-way ANOVA considering the variation in the OD to assess any absorbance differences in the examined materials between the group exposed to the experimental materials and the negative control at the moment of seeding (T0), and the T1, T2, and T3 follow-up resulted statistically significant [2].*

Dunnett's Multiple Comparisons Test	Mean Diff.	95.00% CI of Diff.	Adjusted *p* Value
T0			
CONTROL vs. E	0.000	−0.03112 to 0.03112	>0.9999
CONTROL vs. B	0.000	−0.03112 to 0.03112	>0.9999
CONTROL vs. D	0.000	−0.03112 to 0.03112	>0.9999
CONTROL vs. G	0.000	−0.03112 to 0.03112	>0.9999
CONTROL vs. BIOS	0.000	−0.03112 to 0.03112	>0.9999
T1			
CONTROL vs. E	−0.04433	−0.08196 to −0.006706	0.0293
CONTROL vs. B	0.01500	−0.1319 to 0.1619	0.9411
CONTROL vs. D	−0.06233	−0.3709 to 0.2463	0.6323
CONTROL vs. G	−0.07700	−0.1584 to 0.004411	0.0572
CONTROL vs. BIOS	−0.06733	−0.1283 to −0.006324	0.0383
T2			
CONTROL vs. E	0.1517	−0.1327 to 0.4360	0.1765
CONTROL vs. B	0.06467	−0.01648 to 0.1458	0.0969
CONTROL vs. D	0.02300	−0.03654 to 0.08254	0.4412
CONTROL vs. G	0.07267	−0.1858 to 0.3312	0.4911
CONTROL vs. BIOS	−0.08500	−0.3450 to 0.1750	0.4022
T3			
CONTROL vs. E	0.2557	−0.1434 to 0.6547	0.1567
CONTROL vs. B	0.1223	−0.3039 to 0.5486	0.5478
CONTROL vs. D	0.009333	−0.4114 to 0.4300	0.9999
CONTROL vs. G	−0.01467	−0.4908 to 0.4614	0.9992
CONTROL vs. BIOS	0.03733	−0.3601 to 0.4348	0.9863

Table 4. Dunnett's post hoc multiple comparison results [2].

5.3.2 Morphological Analysis: LM

"LM analysis unveiled a high-density layer of healthy hPLFs in all groups of cells exposed to the materials, with differences between them (Figure 15). At the T1 of the culture, the control group of hPLFs showed small dimensions and a fusiform shape of the cellular body [2].

All the experimental groups showed a more prominent cellular shape compared to the control group, displaying cytoplasmatic extensions towards the biomaterials. Larger cell dimensions were also detected in the positive control group. At T2, the negative control group displayed fusiform cells with opalescence signs. Slightly fusiform cells, characterized by cytoplasmatic prolongations in the proximity of the material, were also observed in hPLFs of group E. Multilayer cells, with a high presence of cytoplasmic processes towards the material, were also detected in group B. Cells characterized by enlarged cellular bodies were observed in D and G groups. A large shape, characterized by cytoplasmatic extensions, was also detected in hPLFs exposed to the Bio-Oss graft. Fusiform morphology was observed in the negative control cells at T3. In contrast, cells of groups E, B, D, and G, and hPLFs of the positive control group Bio-Oss (BIOS)

presented a polygonal shape, appeared densely packed, also displaying cytoplasmatic extensions in the proximity of the biomaterials [2].”

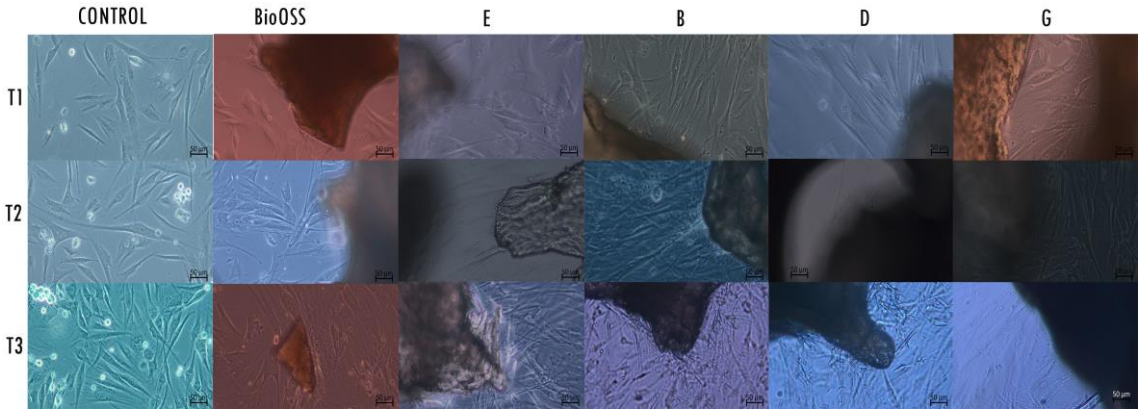

Figure 15. LM images of hPLFs with the examined materials and the negative control at different times. *Magnification 20× [2].*

5.3.3 Morphological Analysis: SEM

“SEM observations (Figure 16) showed that, at T1, the body of fibroblasts exposed to biomaterials E, B, D, and G, and Bio-Oss were enlarged with cytoplasmatic extensions and digitation on the membrane. At T2, the HPLFs in contact with the E biomaterial were flat, while the cells exposed to experiment biomaterial B produced a cytoplasmatic extension towards the biomaterial. Cells exposed to biomaterial D continued thickening, while those exposed to G appeared flat. HPLFs in contact with Bio-Oss were thicker, with cytoplasmatic extensions and digitation on the membrane. At T3, the fibroblast surfaces exposed to E biomaterial appeared flat and covered the bone particles. The surface

morphology of the cells exposed to material B appeared highly dynamic with thick cytoplasmatic prolongation. In contrast, HPLFs exposed to D and G biomaterials showed a flat morphology but covered and incorporated the biomaterial particles. The cells exposed to Bio-Oss continued to appear thick, incorporating bone particles with cytoplasmatic prolongation from the membrane [2].”

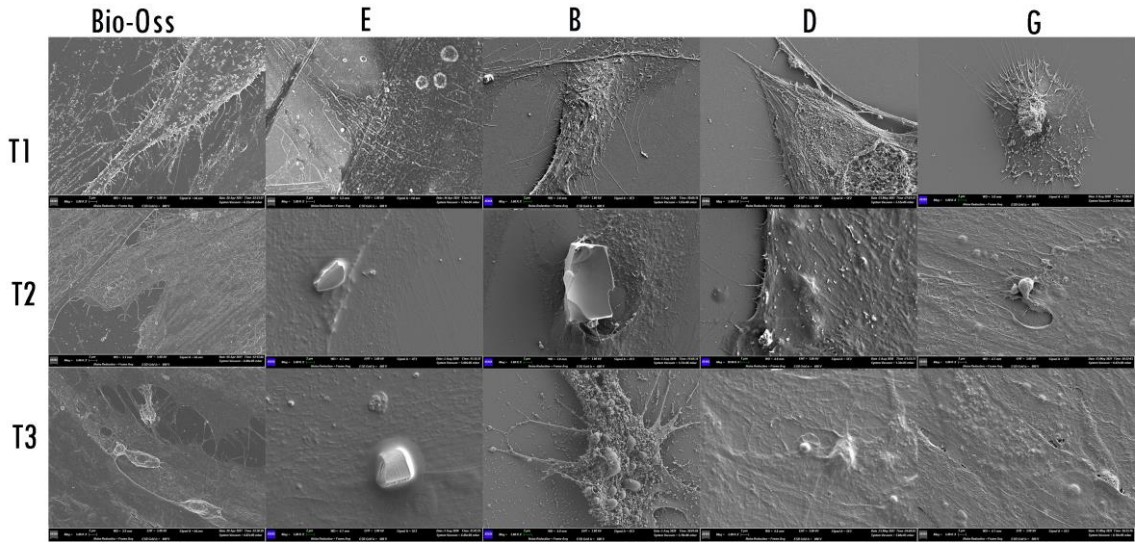

Figure 16. SEM images. *Different reactions of the fibroblasts when exposed to the grafts Bio-Oss, E, B, D, and G at 24 h, 72 h, and 7 days. Magnification: 500× [2].*

5.3.4 Morphological Analysis: CLSM

"The CLSM observations allowed us to assess the status of the nuclei (blue) and the expression and distribution of the actin (red). The nuclei showed an oval or rounded (blue) shape and were well-represented in all samples. The actin (red) staining differed between groups and among the follow-up times. The negative control group showed weakness in the red signal; at the T3 follow-up, the signal slightly increased. At the T1 follow-up, experimental groups E, B, and D showed a strong red signal, which progressively increased at T2 and T3 follow-ups. Actin distribution was observed in the cellular contour, projections, and protrusions [2].

Regarding the fibroblasts exposed to G, the material showed a weak actin signal at the T1 follow-up, mainly present at the contour of the body cells. The G samples started to express a stronger actin signal at T2, distributed in the cytoplasmatic projections; the signal and the distribution increased at the T3 follow-up. Regarding the sample Bio-Oss, the actin signal was expressed at the T1 follow-up and increased in T2 and T3 follow-ups (Figure 17) [2]."

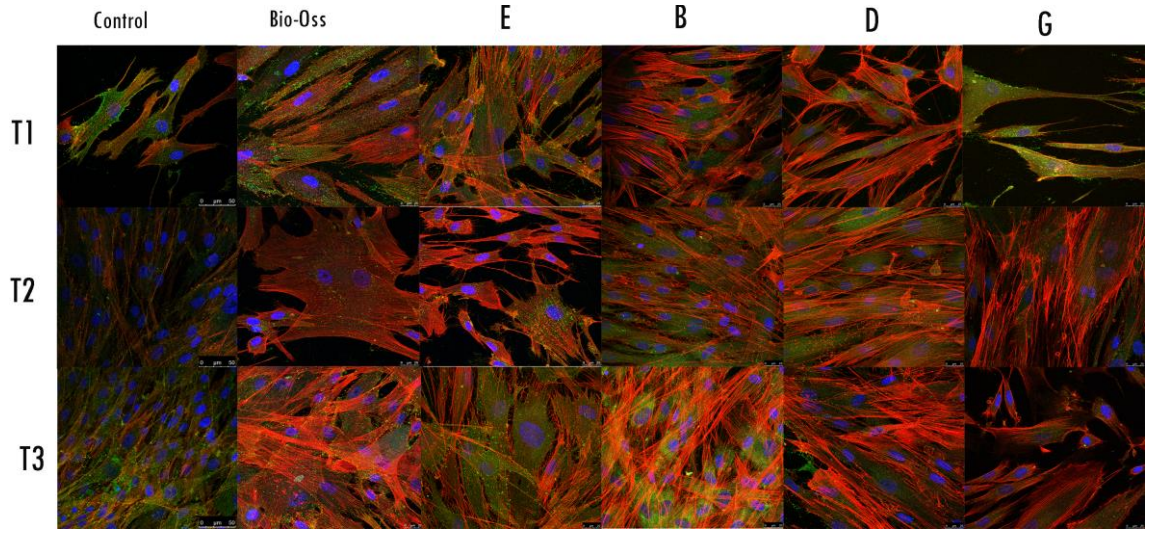

Figure 17. CLSM images showing actin filaments using phalloidin in control and treated fibroblasts marked with CD90 (green) at different follow-up times. *Magnification 63× [2].*

CHAPTER 6 - DISCUSSION

Regenerative medicine is a health science field that restores damaged tissues by exploiting their regenerative potential and providing specific biomolecules and growth factors that trigger and sustain the regenerative process. HPLFs are a fundamental contributor to regenerative dynamics of periodontal tissues and are also involved in immune and inflammatory pathways in periodontal disease [94]. HPLFs in fact are a heterogenous cellular population, characterized by considerable self-renewal capacities and dependent from several soluble factors, which determine their distinct fates [94].

Regarding the biomaterials applied for regenerative purposes, a pivotal role is reserved to APCs. Platelets are important regulators of coagulation, hemostasis, angiogenesis, and tissue regeneration [95], which provide autologous concentrates easy to obtain for experimental and clinical purposes. APCs, which contain a polymer of fibrin matrix with a high concentration of growth factors [17,96,97], are characterized by a high regenerative potential, and are frequently applied in regenerative therapies and interventions [98]. Nevertheless, there is still a challenging debate on the efficacy of APCs' protocols. APCs, derived from a patient's venous blood, are particularly rich in growth factors involved in the binding of receptors of the healing process. Moreover, they also contain cytokines and

anti-inflammatory molecules as a further biological value [99]. The APG, the PRF, and the CGF in fact release growth factor: among them, PDGF, TGF-β, ILGF-1, VEGF, and EGF, which exert a chemotactic activity and regulate differentiation and proliferation in the cellular environment [100]. APCs' regenerative potential is also determined by the timing for the release of growth factors: due to a different timing for fibrin polymerization, the APG is characterized by a quick release of growth factors, while the PRF and CGF by a slow growth factors' release [100]. Moreover, scientific evidence reported the release in the first hour of a significant amount of growth factors by the APG, when compared to the PRF [100].

The regenerative induction is different and based on the application of different materials according to the specific clinical situation. Furthermore, the timing of the growth factor release influences the choice of the material to use regarding performance, as suggested by the pre-determined treatment plan. The APG might be a valid option, when a fast regeneration but no intervention later in time is necessary, instead, the PRF or CGF may represent a better alternative, when several surgical interventions are required. This issue is highlighted by the results of our in vitro study. The XTT assay unveils a difference in the proliferation activity of hPLFs, exposed to three selected APCs at different times.

The PRF showed and intense proliferation at 24h, with a subsequent decrease, as highlighted by XTT assays. This trend could be due to a reduction in the number of platelets and a thick fibrin matrix, occurring with the application of high spin protocol, procedures used in socket preservation or in treating periodontal defects [101].

The application of PRF, associated with an open flap technique, determines a significant reduction of the periodontal depth than at control sites with a difference of 2.17 mm [102]. Furthermore, a lower density characterizes the CGF fibrin matrix, when compared to the PRF: for this reason, the fibrin network is not able to contain a higher volume of platelets and growth factors [103]. The APG instead is characterized by an initial release of growth factors, probably associated with the low density of the fibrin matrix in which the platelets are not trapped [104]. The APG application is also essential for the activation of biomaterials, such as bovine bone grafts, by creating a gel incorporating bone chips, promoting the insertion during interventions for ridge preservation, sinus floor augmentation, or treating mandibular II-degree furcation [105]. Scientific evidence highlighted that the application of APG, combined with bovine bone grafts, determines a lack of closure of the furcation defects, ascribing a limited role of autologous APG as a regenerative material in the periodontal field [106].

Our LM and SEM evidence showed significant morphological changes due to the presence of APCs, which support the proliferation data provided by the XTT assay. The cells' ability to move over the surface of APCs is confirmed by the detected hPLF spreading and differences in the spreading time are probably due to the microenvironment [107], which is sensitive to APCs' physical properties, such as the stiffness and thickness [108]. Furthermore, the cellular activation and interaction with the extracellular environment are confirmed by the increase in cell body dimensions, the polygonal shape, and the presence of cellular projections. These structural and ultrastructural findings unveil a fine balance between motility and adaptive cell adhesion to the APC components. CLSM evidence clarify the LM and SEM observations. CLSM investigates the expression of the most abundant cytoplasmatic protein of eukaryotic cells, actin protein, which performs multiple functions, including morphological changes, signal transduction, and cell motility [109].

A progressive increase and a dynamic distribution of actin prove the cytoskeletal remodeling enhanced by APCs. As highlighted by the controls at 24 h, 72 h, and 7 days, actin expression was physiological and characterized by a stable morphology. Besides, an intense actin expression at all the selected times, with a significant re-organization of

the intracellular actin protein inside the projections was observed in hPLFs cultured with APCs. The induction of proliferation by APCs is confirmed by theseevidence, specifically when combined to the analysis of the nuclei; at the same time, these data proved the cytoskeletal re – organization highlighted by SEM.

Furthermore, actin is a cytoskeletal protein involved in the modification of cellular morphology, movement, and migration of cellular organelles, but it is also the indicator of fibroblast activation [110–112]. Recent study assessed the stimulatory effect of APCs on migration and proliferation of hPLFs [113], supporting their clinical application.

The cytosolic actin is responsible of the development of cellular projections, such as lamellipodia. Moreover, specific cytokines exert in the wound key chemotactic and repairing roles for the subsequent regenerative processes. Specifically, PDGF and TGF-β released during wound healing, promote cellular proliferation, migration, and collagen synthesis in fibroblasts [114,115].

Our structural and ultrastructural evidence unveil the interaction between the chemical-physical properties of the selected APCs and fibroblast activation. All the APCs are suitable for tissue regeneration techniques and showed significant regenerative potential on hPLFs; however, the differences in proliferation, spreading, and fibroblast activation

may determine the choice of the appropriate APC according to specific clinical situations in regenerative periodontal applications.

As regards the bio-morphological reaction of hPLFs to different types of dentinal derivates, our research highlights that different degrees of dentinal mineralization induce distinct cellular reactions. Dentinal derivates are a new class of autologous biomaterial with a considerable regenerative potential. Dentin is an available tissue for dentists, with a versatile chemical composition and interesting embryologic origin [63]. Dentin is composed by a mineral phase (70%), organic matrix (20%), water (10%), and tubule of odontoblasts, embryologically derived from a mesenchymal tissue. Dentin mineral phase included calcium-phosphate molecules, while the organic matrix is formed by collagen I fibers and proteins such as growth factors, such as BMPs. Due to this composition, it is considered a valid grafting material [63]. The development of different protocols, to obtain a granular material similar to the bone tissue, provided an autologous material more available than autologous bone. Mineralized deproteinized dentine and demineralized dentine are valid options obtained by the available machines. These dentinal derivates have a solid 3D structure; demineralized dentin is associated with collagen and BMPs [62].

The application of the mineral part of the body without performing a bone auto-transplant is not new; nevertheless, the commercialization of the machines, which process the tooth is recent, and the reactions of the oral hard tissues to these grafts are still debated [116,117]. Noteworthy, the processing methods cannot defeat the quality issues of the dentinal tissue source. The fibroblast adherence [118] is determined by a clean surface obtained with accurate root scaling and debridement [118] or by laser therapy or photodynamic therapy for selective biofilm [119]. However, the quality of obtained graft might be improved by a pre-treatment of the tooth source.

Dentinal derivates are applied to correct bone defects before implant placements and for alveolar socket preservations. Scientific evidence [97] confirmed the dynamic reaction of post-extractive sites histologically, successively hosting implants filled with mineralized dentin derivates. Specifically, histological observations detected the presence of newly formed bone tissue and the residue of particle dentin [97]. Furthermore, implants' osseointegration was confirmed at the one-year follow-up [97].

Recent clinical trial compared the integration of mineralized dentin and xenograft in post-extractive sites for ridge preservation and implant placements [120]. From a histological point of view, a quantity of newly formed bone in the sites filled with the dentin was

detected, and no differences in the implant therapy outcomes [120]. Other studies histologically evaluated the demineralized dentine graft, derived from the same protocol we applied for TT, placed in post-extractive sites and compared to a graft mixing the demineralized dentine and the mineralized deproteinized bone [121]. After four months of follow - up, there was a higher percentage of newly formed bone in the sites grafted with the dentine than in the sites grafted with the mixed materials, as confirmed by histological evidence [121].

Regarding our in vitro study, a positive response from the hPLFs exposed to the selected materials was observed, with similar reactions with SG, BIOS, and different behavior toward DDP and TT. The mineralized materials induced the thickening of the membrane, related to the mineral content, as a surface reaction, while regarding the response timing, TT showed the best results, considering the proliferation and adhesions at the T2, due to the proteins and induction factors missing in the DDP. However, the cells showed a later response (T3) to the demineralized scaffold.

Furthermore, different mineralization degrees affect fibroblast proliferation. In our study, the distinct types of dentinal derivates determined distinct biological and morphological reactions. All the experimental materials induced a significant proliferation in the hPLFs.

The SG determined a significant growth difference at all the follow-up times. At the T3 follow-up, all the materials, except for the DDP, induced significant growth compared with the negative control. Yeomans et al. [122] highlighted how demineralized dentin placed in bone sites induced the formation of bone earlier than the mineralized dentin. Some studies [123] found BMPs in the demineralized dentin as potential cellular inductive factors. Blum et al. [124] confirmed this issue, suggesting that the demineralization of the dentin promotes the release of the cellular induction. Besides, demineralized dentin provides a suitable carrier for inductive growth factors, differently from mineralized materials, which request more time to degrade; at the same time, the mineral content influences cellular activity.

Our data align with the findings reported in the literature [125,126]. As Alliot-Licht et al. [127] reported , HA causes a first initial delay in the proliferation activity of the hPLFs and an increase on the third day of in vitro culture. Moreover, LM and SEM observations unveil critical structural and ultrastructural reactions toward a different type of dentinal graft: the observed changes in the shape of the fibroblasts suggest a positive reaction to the material exposure in terms of cellular activation, as confirmed by the dimensional

increase in the cell body, the polygonal morphology, and the development of several cellular digitations towards the material granules.

SEM images highlighted the fibroblast membrane reaction to the different types of dentinal derivates and the positive control. HPLFs are characterized by thickening their membrane in the presence of SG and BIOS, while hPLFs exposed to DDP and TT reacted by flattening their membrane. These ultrastructural evidence are consistent with those in the literature. Recent studies [128] highlighted how the deproteinized mineralized dentin enhance the elongation of human dental pulp stem cells adhering to the graft surface. As reported in the literature [62], the demineralized dentin induced adhesion of osteoblasts on the surfaces of the tested graft. However, the authors did not observe a thickening of the membrane [62]. CLSM observation confimed the LM and SEM data. A progressive increase and a dynamic expression and distribution of vinculin, actin, and integrin are suggestive of the cytoskeletal reaction to the experimental material. Integrins are a family of transmembrane adhesion receptors composed of non-covalent heterodimeric complexes involving α and β chains, which regulate different cellular effects in physiological and pathological situations [129]. A growing body of evidence highlight that integrin αVβ3 plays a pivotal role in angiogenesis and migration processes [130].

Instead, vinculin is an actin-binding protein that regulates cell adhesion by directly binding to actin, stimulating its polymerization, and recruiting actin- remodeling proteins [131]. These cytoskeletal markers were expressed in all experimental and control materials, but with difference depending on the follow-up times: at 24 h, actin filaments were visible in all materials. Vinculin and integrin are primarily expressed in the DDP and BIOS material, suggesting an earlier adhesion of the fibroblasts [132,133]. At 72 h, the DDP and TT showed stronger vinculin and integrin signals than the SG and BIOS, characterized by a well-defined actin expression, suggesting the reorganization of the cytoskeletal components. Actin is a cytoskeletal protein involved in the morphological changes of the cells and the movement of cellular organelles; therefore, it is a signal of the activation of fibroblasts [108,111,112]. At the 7-day follow-up, vinculin was highly expressed in fibroblasts exposed to the DDP material, while actin expression was more detectable in fibroblasts exposed to the other materials. Our results are supported by previous evidence in the literature: Hakkinen et al. [134] showed different fibroblast reactions in terms of migration and adhesion in 2D cultures, underlining how actin plays a pivotal role in cellular migration and adhesion to the ECM. For these reasons, the mineralization degree and the protein content affect the hPLF reactions in terms of

proliferation, adhesion, and migration. The DDP, which provides a demineralized scaffold, is associated to an early adhesion of the cells. Moreover, the SG which provides a solid mineral scaffold, showed a similar expression of the adhesion protein at the middle point (72 h), to the BIOS and TT, which provide a demineralized scaffold with BMPs releases. Indeed, the DDP showed a late adhesion response of the fibroblasts at 7 days follow-up.

Finally, our research investigates the morphological and biological reaction of hPLFs to different bovine bone grafts treated with low-temperature deproteinization protocol. Our results highlighted how the physiochemical properties of these biomaterials, given by the manufacturing process, play a pivotal role in cellular stimulation. Moreover, the quality of the regenerative properties of grafting materials relies on their physiochemical compositions, with significant effects on cellular induction, conductivity, stability of the scaffold, and degradation mechanisms [135]. Xenografts are still a valid option for oral surgery and periodontal regeneration procedures, even if some of their properties are still debated. Specifically, several studies have analyzed the effect of the size of the granules in bone tissue regeneration procedures [136,137]. Scientific evidence assessed that small granules (size 0.4mm) are resorbed faster than large granules, leading to the synthesis of

osteoid tissue [137]. Other studies confirmed the linkage between the size of the particles, the properties' surface, and the remodeling process, by using a different type of graft [136]. Leiblein et al. reported the effects of the particle's sizes of grafts on the regenerative process, specifically regarding inflammation and bone formation [138].

Moreover, the quality of the collected bone particles also impacts on the regenerative process: the trabecular structure, which characterizes cancellous bone grafts, induces new vascular supply and graft integration [139]. However, due to a weak structural stability, the trabecular structure is not able in supporting the load [139]. Stability and resistance to compression loads are also provided by cortico-cancellous bone, which also induces cellular proliferation in the trabecular structures, as reported by Mazzoni et al. [140].

Furthermore, treatments to remove prion and animal protein from bovine-derived grafts were also performed and these procedures, both high temperature and chemical treatments, impact on the structure, the surface, the mineral content and stability of the biomaterials. Indeed, xenografts submitted to higher temperatures make products slowly absorbable [141]. Recent studies compared the resorption process of two biomaterials in vivo, subjected to low or high temperature protocols [142]. A lower ratio of mineral phase (Ca/P), collagen, higher porosity, and a higher capacity to be degraded was found in

xenograft treated with low temperature compared to the graft treated with high temperature [143]. Block et al., instead, examined the stability of high-temperature biomaterial, applying an animal origin over an extended period: the authors reported that the application of this type of material is not associated to a long-term stability in ridge augmentation [143]. Moreover, recent evidence highlighted a low cellular proliferation of a pre-osteoblastic line in contact with two types of xenografts (one processed with high temperature and chemical solvents, and the other not), reporting no differences at the T2 follow-up [144]. This study demonstrated how the temperature treatment impact on the porosity and cellular capacity of the material's penetration, by influencing the cellular viability tests [144].

Our study describes the cellular reaction of hPLFs, towards biomaterial of different sizes, not submitted to high temperature, from a proliferative to a morphological point of view. XTT data highlighted a positive growth in all follow-ups and experimental materials, with no difference and considering their size and composition. Morphological data highlighted the qualitative differences in the observed in vitro culture. Furthermore, LM observations detected structural modifications in the cellular shapes of all exposed samples. SEM observations highlighted a progressive thickening of the membrane and the development

of cellular projections and extension towards the biomaterial in hPLFs exposed to the cortical and cancellous granules with a size between 0.25 and 1 mm (sample B) and not exposed to chemical deproteinization. HPLFs exposed to the other three samples, E (cancellous granules with a size between 0.25 and 1 mm), D (cortico-cancellous granules with a size between 0.25 and 1 mm), and G (cancellous granules with a size between 1 and 2 mm), showed a progressive flattening of the membrane and the development of external projections. Besides, SEM observations detected a different cell culture behavior when exposed to the positive control material (cancellous granules with a size between 0.25 and 1 mm exposed to high temperature and chemical deproteinization), with a progressive thickening of the membrane in the considered follow-ups. CLSM images support SEM findings and unveil how the actin signal appears stronger in B and D samples than in E and G samples in T1 and T2 follow-ups.

Moreover, CLSM observations highlighted a progressive increase in the actin signal from T1 to T3, by confirming the stimulation of the membrane from the positive control material. This progressive increase in the actin signal, combined with structural and ultrastructural modifications in the cellular shape, suggest how the xenografts stimulated a reorganization of the cytosolic actin and cytoskeleton modifications. Finally, actin

protein is a definitive marker of fibroblast activation, involved in shape modifications, migration, and cell organelle movements [111].

As regards the effects of graft chemical deproteinization on cellular morphology, chemical treatment is another critical factor influencing the final properties of the product. The WHO guidelines for prions' inactivation recommend the application of NaOCl and NaOH [145]. Chemical deproteinization is essential to remove prions and animal proteins, which might result in an immunological reaction by the host organism, with interesting effects on the properties of the graft. Therefore, some studies reported how xenografts deproteinised with pepsin have more osteogenic properties than those submitted to H_2O_2 deproteinization [146].

Bi et al. [147] analyzed the cancellous bone treated with NaOH, highlighting how these xenografts presented surface fissures, the high organic content of Ca and P, lower resistance to mechanical stress, low trabecular thickness, and low cytocompatibility.

Our data are consistent with previous evidence, as shown by the XTT proliferation assays and morphological observations. Bonferroni post hoc analysis did not show any significant differences between the experimental materials submitted to the chemical process of deproteinization. LM observations detected an increase in cellular body sizes

and a modification into a polygonal morphology, confirmed by SEM examinations showing the development of cellular projections towards experimental material B. Moreover, these data were supported by the expression of a strong actin signal in CLSM investigations. Low temperatures and lack of exposure to the chemical deproteinization promotes the cytosolic actin, lamellipodia development, cellular membrane's thickening, and a possible cellular migration towards the biomaterials. The possible clinical implications of using xenografts processed with low temperatures and not chemically exposed in periodontal defects regeneration are a faster healing process due to important conduction and stimulation at the cellular level.

CHAPTER 7 - CONCLUSIONS

According to our bio – morphological evidence, APCs are suitable as scaffold materials for fibroblast cell culture. These findings suggest that APCs may be reliable materials for guided tissue regeneration techniques in periodontology.

As regards dentinal derivates, different degrees of dentinal mineralization promote different cellular behaviors in terms of proliferation, migration, and adhesion (as shown by the proliferative assays). Furthermore, LM and SEM examinations highlighted the expression of cytoskeletal markers and the change in the external morphology. The knowledge of the inductive and conductive effects of the degree of mineralization of the dentine on the cellular behavior will help the clinician in the choice of the type of dentine derivates material according to the required clinical situation.

Despite the described limitations, our biological and morphological results indicated that all xenografts not submitted to high temperature showed important cellular stimulations, with specific and interesting interactions with the material not chemically treated. These evidence also suggest that alternative deproteinization protocols are less invasive for making xenografts compatible and might improve the osteoconductive properties in

regeneration interventions. However, animal model experiments and randomized clinical trials are needed to confirm these results.

References

1. Murphy, C.; O'Brien, F.; Little, D.; Schindeler, A. Cell-Scaffold Interactions in the Bone Tissue Engineering Triad. *Eur Cell Mater* **2013**, *26*, 120–132, doi:10.22203/eCM.v026a09.

2. Bianchi, S.; Bernardi, S.; Mattei, A.; Cristiano, L.; Mancini, L.; Torge, D.; Varvara, G.; Macchiarelli, G.; Marchetti, E. Morphological and Biological Evaluations of Human Periodontal Ligament Fibroblasts in Contact with Different Bovine Bone Grafts Treated with Low-Temperature Deproteinisation Protocol. *Int J Mol Sci* **2022**, *23*, doi:10.3390/ijms23095273.

3. Abdollahiyan, P.; Oroojalian, F.; Mokhtarzadeh, A. The Triad of Nanotechnology, Cell Signalling, and Scaffold Implantation for the Successful Repair of Damaged Organs: An Overview on Soft-Tissue Engineering. *J Control Release* **2021**, *332*, 460–492, doi:10.1016/j.jconrel.2021.02.036.

4. Jacques, E.; Suuronen, E.J. The Progression of Regenerative Medicine and Its Impact on Therapy Translation. *Clin Transl Sci* **2020**, *13*, 440–450, doi:10.1111/cts.12736.

5. Krishani, M.; Shin, W.Y.; Suhaimi, H.; Sambudi, N.S. Development of Scaffolds from Bio-Based Natural Materials for Tissue Regeneration Applications: A Review. *Gels* **2023**, *9*, 100, doi:10.3390/gels9020100.

6. Terzic, A.; Pfenning, M.A.; Gores, G.J.; Harper, C.M. Regenerative Medicine Build-Out. *Stem Cells Transl Med* **2015**, *4*, doi:10.5966/sctm.2015-0275.

7. Ciccocioppo, R.; Cantore, A.; Chaimov, D.; Orlando, G. Regenerative Medicine: The Red Planet for Clinicians. *Intern Emerg Med* **2019**, *14*, 911–921, doi:10.1007/s11739-019-02126-z.

8. Tirone, M.; Tran, N.L.; Ceriotti, C.; Gorzanelli, A.; Canepari, M.; Bottinelli, R.; Raucci, A.; di Maggio, S.; Santiago, C.; Mellado, M.; et al. High Mobility Group Box 1 Orchestrates Tissue Regeneration via CXCR4. *J Exp Med* **2018**, *215*, doi:10.1084/jem.20160217.

9. Julier, Z.; Park, A.J.; Briquez, P.S.; Martino, M.M. Promoting Tissue Regeneration by Modulating the Immune System. *Acta Biomater* **2017**, *53*, 13–28, doi:10.1016/j.actbio.2017.01.056.

10. Yamada, S.; Shanbhag, S.; Mustafa, K. Scaffolds in Periodontal Regenerative Treatment. *Dent Clin North Am* **2022**, *66*, 111–130, doi:10.1016/j.cden.2021.06.004.

11. Dudas, M.; Wysocki, A.; Gelpi, B.; Tuan, T.-L. Memory Encoded Throughout Our Bodies: Molecular and Cellular Basis of Tissue

Regeneration. *Pediatr Res* **2008**, *63*, 502–512, doi:10.1203/PDR.0b013e31816a7453.

12. Ivanovski, S.; Vaquette, C.; Gronthos, S.; Hutmacher, D.W.; Bartold, P.M. Multiphasic Scaffolds for Periodontal Tissue Engineering. *J Dent Res* **2014**, *93*, 1212–1221, doi:10.1177/0022034514544301.

13. Park, C.; Kim, K.-H.; Lee, Y.-M.; Seol, Y.-J. Advanced Engineering Strategies for Periodontal Complex Regeneration. *Materials* **2016**, *9*, 57, doi:10.3390/ma9010057.

14. Keith, J.D.; Petrungaro, P.; Leonetti, J.A.; Elwell, C.W.; Zeren, K.J.; Caputo, C.; Nikitakis, N.G.; Schöpf, C.; Warner, M.M. Clinical and Histologic Evaluation of a Mineralized Block Allograft: Results from the Developmental Period (2001-2004). *Int J Periodontics Restorative Dent* **2006**, *26*.

15. Belal, M.H.; Al-Noamany, F.A.; El-Tonsy, M.M.; El-Guindy, H.M.; Ishikawa, I. Treatment of Human Class II Furcation Defects Using Connective Tissue Grafts, Bioabsorbable Membrane, and Resorbable Hydroxylapatite: A Comparative Study. *J Int Acad Periodontol* **2005**, *7*.

16. Chu, K.T.; Oshida, Y.; Hancock, E.B.; Kowolik, M.J.; Barco, T.; Zunt, S.L. Hydroxyapatite/PMMA Composites as Bone Cements. *Biomed Mater Eng* **2004**, *14*.

17. Bernardi, S.; Di Girolamo, M.; Necozione, S.; Continenza, M.A.; Cutilli, T. Antiresorptive Drug-Related Osteonecrosis of the Jaws, Literature Review and 5 Years of Experience. *Musculoskelet Surg* **2019**, *103*, doi:10.1007/s12306-018-0548-6.

18. Bernardi, S.; Macchiarelli, G.; Bianchi, S. Autologous Materials in Regenerative Dentistry: Harvested Bone, Platelet Concentrates and Dentin Derivates. *Molecules* **2020**, *25*, doi:10.3390/molecules25225330.

19. Spanemberg, J.C.; Cardoso, J.A.; Slob, E.M.G.B.; López-López, J. Quality of Life Related to Oral Health and Its Impact in Adults. *J Stomatol Oral Maxillofac Surg* **2019**, *120*, 234–239, doi:10.1016/j.jormas.2019.02.004.

20. Liu, X.; Zhao, K.; Gong, T.; Song, J.; Bao, C.; Luo, E.; Weng, J.; Zhou, S. Delivery of Growth Factors Using a Smart Porous Nanocomposite Scaffold to Repair a Mandibular Bone Defect. *Biomacromolecules* **2014**, *15*, doi:10.1021/bm401911p.

21. Anitua, E.; Alkhraist, M.; Piñas, L.; Begoña, L.; Orive, G. Implant Survival and Crestal Bone Loss Around Extra-Short Implants Supporting a Fixed Denture: The Effect of Crown Height Space, Crown-to-Implant Ratio, and Offset Placement of the Prosthesis. *Int J Oral Maxillofac Implants* **2014**, *29*, doi:10.11607/jomi.3404.

22. Antonoglou, G.; Stavropoulos, A.; Samara, M.; Ioannidis, A.; Benic, G.; Papageorgiou, S.; Sándor, G. Clinical Performance of Dental Implants

Following Sinus Floor Augmentation: A Systematic Review and Meta-Analysis of Clinical Trials with at Least 3 Years of Follow-Up. *Int J Oral Maxillofac Implants* **2018**, *33*, doi:10.11607/jomi.6417.

23. Raghoebar, G.M.; Onclin, P.; Boven, G.C.; Vissink, A.; Meijer, H.J.A. Long-Term Effectiveness of Maxillary Sinus Floor Augmentation: A Systematic Review and Meta-Analysis. *J Clin Periodontol* **2019**, *46*, doi:10.1111/jcpe.13055.

24. Park, W.B.; Kang, K.L.; Han, J.Y. Factors Influencing Long-Term Survival Rates of Implants Placed Simultaneously with Lateral Maxillary Sinus Floor Augmentation: A 6- to 20-Year Retrospective Study. *Clin Oral Implants Res* **2019**, *30*, doi:10.1111/clr.13505.

25. Bernardi, S.; Gatto, R.; Severino, M.; Botticelli, G.; Caruso, S.; Rastelli, C.; Lupi, E.; Quiroz Roias, A.; Iacomino, E.; Falisi, G. Short versus Longer Implants in Mandibular Alveolar Ridge Augmented Using Osteogenic Distraction: One-Year Follow-up of a Randomized Split-Mouth Trial. *J Oral Implantol* **2018**, *44*, 184–191, doi:10.1563/aaid-joi-D-16-00216.

26. Aghaloo, T.; Misch, C.; Lin, G.-H.; Iacono, V.; Wang, H.-L. Bone Augmentation of the Edentulous Maxilla for Implant Placement: A Systematic Review. *Int J Oral Maxillofac Implants* **2017**, *31*, doi:10.11607/jomi.16suppl.g1.

27. Arjunan, A.; Baroutaji, A.; Robinson, J.; Praveen, A.S.; Pollard, A.; Wang, C. Future Directions and Requirements for Tissue Engineering Biomaterials. In *Encyclopedia of Smart Materials*; **2021**.

28. Mas-Moruno, C.; Su, B.; Dalby, M.J. Multifunctional Coatings and Nanotopographies: Toward Cell Instructive and Antibacterial Implants. *Adv Healthc Mater* **2019**, *8*, 1801103, doi:10.1002/adhm.201801103.

29. Beyene, Z.; Ghosh, R. Effect of Zinc Oxide Addition on Antimicrobial and Antibiofilm Activity of Hydroxyapatite: A Potential Nanocomposite for Biomedical Applications. *Mater Today Commun* **2019**, *21*, doi:10.1016/j.mtcomm.2019.100612.

30. Kumar, A.; Kargozar, S.; Baino, F.; Han, S.S. Additive Manufacturing Methods for Producing Hydroxyapatite and Hydroxyapatite-Based Composite Scaffolds: A Review. *Front Mater* **2019**, *6*, doi:10.3389/fmats.2019.00313.

31. Nazeer, M.A.; Onder, O.C.; Sevgili, I.; Yilgor, E.; Kavakli, I.H.; Yilgor, I. 3D Printed Poly(Lactic Acid) Scaffolds Modified with Chitosan and Hydroxyapatite for Bone Repair Applications. *Mater Today Commun* **2020**, *25*, doi:10.1016/j.mtcomm.2020.101515.

32. Arjunan, A.; Baroutaji, A.; Praveen, A.S.; Robinson, J.; Wang, C. Classification of Biomaterial Functionality. In *Encyclopedia of Smart Materials*; **2021**.

33. Zhang, H.Y.; Jiang, H.B.; Kim, J.E.; Zhang, S.X.; Kim, K.M.; Kwon, J.S. Bioresorbable Magnesium-Reinforced PLA Membrane for Guided Bone/Tissue Regeneration. *J Mech Behav Biomed Mater* **2020**, *112*, doi:10.1016/j.jmbbm.2020.104061.

34. Zheng, Y.F.; Gu, X.N.; Witte, F. Biodegradable Metals. *Materials Science and Engineering: R: Reports* **2014**, *77*, 1–34, doi:10.1016/j.mser.2014.01.001.

35. Li, Y.; Pavanram, P.; Zhou, J.; Lietaert, K.; Taheri, P.; Li, W.; San, H.; Leeflang, M.A.; Mol, J.M.C.; Jahr, H.; et al. Additively Manufactured Biodegradable Porous Zinc. *Acta Biomater* **2020**, *101*, doi:10.1016/j.actbio.2019.10.034.

36. Kasuga, T. Coatings for Metallic Biomaterials. In *Metals for Biomedical Devices*; **2019**.

37. Makvandi, P.; Ali, G.W.; della Sala, F.; Abdel-Fattah, W.I.; Borzacchiello, A. Hyaluronic Acid/Corn Silk Extract Based Injectable Nanocomposite: A Biomimetic Antibacterial Scaffold for Bone Tissue Regeneration. *Mater Sci Eng C* **2020**, *107*, doi:10.1016/j.msec.2019.110195.

38. Regulation (EU) 2017/745 of the European Parliament and of the Council of 5 April 2017 – on Medical Devices, Amending Directive 2001/83/EC, Regulation (EC) No 178/2002 and Regulation (EC) No 1223/2009 and Repealing Council Directives 90/385/EEC and 93/42/EEC.

39. Huang, B.; Yuan, Y.; Liu, C. Biomaterial-Guided Immobilization and Osteoactivity of Bone Morphogenetic Protein-2. *Appl Mater Today* **2020**, *19*, 100599, doi:10.1016/j.apmt.2020.100599.

40. Ebrahimi, M. Standardization and Regulation of Biomaterials. In *Handbook of Biomaterials Biocompatibility*; Elsevier, **2020**; pp. 251–265.

41. Melcher, A.H. On the Repair Potential of Periodontal Tissues. *J Periodontol* **1976**, *47*, 256–260, doi:10.1902/jop.1976.47.5.256.

42. Urban, I.A.; Monje, A. Guided Bone Regeneration in Alveolar Bone Reconstruction. *Oral Maxillofac Surg Clin North Am* **2019**, *31*, 331–338, doi:10.1016/j.coms.2019.01.003.

43. Cucchi, A.; Sartori, M.; Parrilli, A.; Aldini, N.N.; Vignudelli, E.; Corinaldesi, G. Histological and Histomorphometric Analysis of Bone Tissue after Guided Bone Regeneration with Non-Resorbable Membranes vs Resorbable Membranes and Titanium Mesh. *Clin Implant Dent Relat Res* **2019**, *21*, doi:10.1111/cid.12814.

44. García-Gareta, E.; Coathup, M.J.; Blunn, G.W. Osteoinduction of Bone Grafting Materials for Bone Repair and Regeneration. *Bone* **2015**, *81*, 112–121, doi:10.1016/j.bone.2015.07.007.

45. Sanz, M.; Dahlin, C.; Apatzidou, D.; Artzi, Z.; Bozic, D.; Calciolari, E.; de Bruyn, H.; Dommisch, H.; Donos, N.; Eickholz, P.; et al. Biomaterials and Regenerative Technologies Used in Bone Regeneration in the Craniomaxillofacial Region: Consensus Report of Group 2 of the 15th European Workshop on Periodontology on Bone Regeneration. *J Clin Periodontol* **2019**, *46*, doi:10.1111/jcpe.13123.

46. Camps-Font, O.; Burgueño-Barris, G.; Figueiredo, R.; Jung, R.E.; Gay-Escoda, C.; Valmaseda-Castellón, E. Interventions for Dental Implant Placement in Atrophic Edentulous Mandibles: Vertical Bone Augmentation and Alternative Treatments. A Meta-Analysis of Randomized Clinical Trials. *J Periodontol* **2016**, *87*, doi:10.1902/jop.2016.160226.

47. Sheikh, Z.; Hamdan, N.; Abdallah, M.-N.; Glogauer, M.; Grynpas, M. Natural and Synthetic Bone Replacement Graft Materials for Dental and Maxillofacial Applications. In *Advanced Dental Biomaterials*; Elsevier, **2019**; pp. 347–376.

48. Moussa, N.T.; Dym, H. Maxillofacial Bone Grafting Materials. *Dent Clin North Am* **2020**, *64*, 473–490, doi:10.1016/j.cden.2019.12.011.

49. Wortmann, D.E.; Klein-Nulend, J.; van Ruijven, L.J.; Vissink, A.; Raghoebar, G.M.; Schortinghuis, J. Histomorphometric and Micro-CT Analyses of Calvarial Bone Grafts Used to Reconstruct the Extremely Atrophied Maxilla. *Clin Implant Dent Relat Res* **2020**, *22*, doi:10.1111/cid.12936.

50. Bernardi, S.; Mummolo, S.; Tecco, S.; Continenza, M.A.; Marzo, G. Histological Characterization of Sacco's Concentrated Growth Factors Membrane. *Int J Morphol* **2017**, *35*, doi:10.4067/s0717-95022017000100019.

51. Pinchi, V.; Varvara, G.; Pradella, F.; Focardi, M.; Donati, M.; Norelli, G. Analysis of Professional Malpractice Claims in Implant Dentistry in Italy from Insurance Company Technical Reports, 2006 to 2010. *Int J Oral Maxillofac Implants* **2014**, *29*, doi:10.11607/jomi.3486.

52. Al-Moraissi, E.A.; Alkhutari, A.S.; Abotaleb, B.; Altairi, N.H.; Del Fabbro, M. Do Osteoconductive Bone Substitutes Result in Similar Bone Regeneration for Maxillary Sinus Augmentation When Compared to Osteogenic and Osteoinductive Bone Grafts? A Systematic Review and Frequentist Network Meta-Analysis. *Int J Oral Maxillofac Surg* **2020**, *49*, 107–120, doi:10.1016/j.ijom.2019.05.004.

53. Pocaterra, A.; Caruso, S.; Bernardi, S.; Scagnoli, L.; Continenza, M.A.; Gatto, R. Effectiveness of Platelet-Rich Plasma as an Adjunctive Material to Bone Graft: A Systematic Review and Meta-Analysis of Randomized Controlled Clinical Trials. *Int J Oral Maxillofac Surg* **2016**, *45*, 1027–1034, doi:10.1016/j.ijom.2016.02.012.

54. Scarano, A.; Ceccarelli, M.; Marchetti, M.; Piattelli, A.; Mortellaro, C. Soft Tissue Augmentation with Autologous Platelet Gel and β -TCP: A Histologic and Histometric Study in Mice. *Biomed Res Int* **2016**, *2016*, doi:10.1155/2016/2078104.

55. Franco, D.; Franco, T.; Angélica Maria Schettino; João Medeiros Tavares Filho; Vendramin, F.S. Protocol for Obtaining Platelet-Rich Plasma (PRP), Platelet-Poor Plasma (PPP), and Thrombin for Autologous Use. *Aesthetic Plast Surg* **2012**, *36*, doi:10.1007/s00266-012-9957-3.

56. Choukroun, J.; Diss, A.; Simonpieri, A.; Girard, M.O.; Schoeffler, C.; Dohan, S.L.; Dohan, A.J.J.; Mouhyi, J.; Dohan, D.M. Platelet-Rich Fibrin (PRF): A Second-Generation Platelet Concentrate. Part IV: Clinical Effects on Tissue Healing. *Oral Surg Oral Med Oral Pathol Oral Radiol Endod* **2006**, *101*, doi:10.1016/j.tripleo.2005.07.011.

57. Choukroun, J.; Diss, A.; Simonpieri, A.; Girard, M.O.; Schoeffler, C.; Dohan, S.L.; Dohan, A.J.J.; Mouhyi, J.; Dohan, D.M. Platelet-Rich Fibrin (PRF): A Second-Generation Platelet Concentrate. Part V: Histologic Evaluations of PRF Effects on Bone Allograft Maturation in Sinus Lift. *Oral Surg Oral Med Oral Pathol Oral Radiol Endod* **2006**, *101*, doi:10.1016/j.tripleo.2005.07.012.

58. Rodella, L.F.; Favero, G.; Boninsegna, R.; Buffoli, B.; Labanca, M.; Scarì, G.; Sacco, L.; Batani, T.; Rezzani, R. Growth Factors, CD34 Positive Cells, and Fibrin Network Analysis in Concentrated Growth Factors Fraction. *Microsc Res Tech* **2011**, *74*, doi:10.1002/jemt.20968.

59. Marchetti, E.; Mancini, L.; Bernardi, S.; Bianchi, S.; Cristiano, L.; Torge, D.; Marzo, G.; Macchiarelli, G. Evaluation of Different Autologous Platelet Concentrate Biomaterials: Morphological and Biological Comparisons and Considerations. *Materials* **2020**, *13*, doi:10.3390/ma13102282.

60. Miron, R.J.; Zucchelli, G.; Pikos, M.A.; Salama, M.; Lee, S.; Guillemette, V.; Fujioka-Kobayashi, M.; Bishara, M.; Zhang, Y.; Wang, H.-L.; et al. Use of Platelet-Rich Fibrin in Regenerative Dentistry: A Systematic Review. *Clin Oral Investig* **2017**, *21*, 1913–1927, doi:10.1007/s00784-017-2133-z.

61. Xiao, Y.-T.; Xiang, L.-X.; Shao, J.-Z. Bone Morphogenetic Protein. *Biochem Biophys Res Commun* **2007**, *362*, 550–553, doi:10.1016/j.bbrc.2007.08.045.

62. Bono, N.; Tarsini, P.; Candiani, G. Demineralized Dentin and Enamel Matrices as Suitable Substrates for Bone Regeneration. *J Appl Biomater Funct Mater* **2017**, *15*, doi:10.5301/jabfm.5000373.

63. Calvo-Guirado, J.L.; Montilla, A.B.; De Aza, P.N.; Fernández-Domínguez, M.; Gehrke, S.A.; Cegarra-Del Pino, P.; Mahesh, L.; Pelegrine, A.A.; Aragoneses, J.M.; de Val, J.E.M.S. Particulated, Extracted Human Teeth Characterization by SEM-EDX Evaluation as a Biomaterial for Socket

Preservation: An in Vitro Study. *Materials* **2019**, *12*, doi:10.3390/ma12030380.

64. Gual-Vaques, P.; Polis-Yanes, C.; Estrugo-Devesa, A.; Ayuso-Montero, R.; Mari-Roig, A.; Lopez-Lopez, J. Autogenous Teeth Used for Bone Grafting: A Systematic Review. *Med Oral Patol Oral Cir Bucal* **2017**, *23*, 0–0, doi:10.4317/medoral.22197.

65. Koga, T.; Minamizato, T.; Kawai, Y.; Miura, K.I.; Takashi, I.; Nakatani, Y.; Sumita, Y.; Asahina, I. Bone Regeneration Using Dentin Matrix Depends on the Degree of Demineralization and Particle Size. *PLoS One* **2016**, *11*, doi:10.1371/journal.pone.0147235.

66. Kao, K.; Kim, D.M.; Kuan-Te Ho, D. Clinical Maxillary Sinus Elevation Surgery, First Edition. Edited by Daniel W 13 Choices of Bone Graft Materials Bone Grafting Materials Overview; **2014**.

67. Ng, V.Y. Risk of Disease Transmission With Bone Allograft. *Orthopedics* **2012**, *35*, 679–681, doi:10.3928/01477447-20120725-04.

68. Homayounfar, N.; Khan, M.M.; Ji, Y.; Khoury, Z.H.; Oates, T.W.; Goodlett, D.R.; Chellaiah, M.; Masri, R. The Effect of Embryonic Origin on the Osteoinductive Potential of Bone Allografts. *J Prosthet Dent* **2019**, *121*, doi:10.1016/j.prosdent.2018.09.003.

69. Kämmerer, P.W.; Tunkel, J.; Götz, W.; Würdinger, R.; Kloss, F.; Pabst, A. The Allogeneic Shell Technique for Alveolar Ridge Augmentation: A Multicenter Case Series and Experiences of More than 300 Cases. *Int J Implant Dent* **2022**, *8*, 48, doi:10.1186/s40729-022-00446-y.

70. Solakoglu, Ö.; Götz, W.; Heydecke, G.; Schwarzenbach, H. Histological and Immunohistochemical Comparison of Two Different Allogeneic Bone Grafting Materials for Alveolar Ridge Reconstruction: A Prospective Randomized Trial in Humans. *Clin Implant Dent Relat Res* **2019**, *21*, doi:10.1111/cid.12824.

71. Winkler, T.; Sass, F.A.; Duda, G.N.; Schmidt-Bleek, K. A Review of Biomaterials in Bone Defect Healing, Remaining Shortcomings and Future Opportunities for Bone Tissue Engineering. *Bone Joint Res* **2018**, *7*, 232–243, doi:10.1302/2046-3758.73.BJR-2017-0270.R1.

72. Fukuba, S.; Okada, M.; Nohara, K.; Iwata, T. Alloplastic Bone Substitutes for Periodontal and Bone Regeneration in Dentistry: Current Status and Prospects. *Materials* **2021**, *14*, doi:10.3390/ma14051096.

73. Zou, W.; Li, X.; Li, N.; Guo, T.; Cai, Y.; Yang, X.; Liang, J.; Sun, Y.; Fan, Y. A Comparative Study of Autogenous, Allograft and Artificial Bone Substitutes on Bone Regeneration and Immunotoxicity in Rat Femur Defect Model. *Regen Biomater* **2021**, *8*, doi:10.1093/rb/rbaa040.

74. Tournier, P.; Guicheux, J.; Paré, A.; Maltezeanu, A.; Blondy, T.; Veziers, J.; Vignes, C.; André, M.; Lesoeur, J.; Barbeito, A.; et al. A Partially

Demineralized Allogeneic Bone Graft: In Vitro Osteogenic Potential and Preclinical Evaluation in Two Different Intramembranous Bone Healing Models. *Sci Rep* **2021**, *11*, doi:10.1038/s41598-021-84039-6.

75. Temmerman, A.; Cortellini, S.; van Dessel, J.; de Greef, A.; Jacobs, R.; Dhondt, R.; Teughels, W.; Quirynen, M. Bovine-Derived Xenograft in Combination with Autogenous Bone Chips versus Xenograft Alone for the Augmentation of Bony Dehiscences around Oral Implants: A Randomized, Controlled, Split-Mouth Clinical Trial. *J Clin Periodontol* **2020**, *47*, doi:10.1111/jcpe.13209.

76. Sicari, B.M.; Johnson, S.A.; Siu, B.F.; Crapo, P.M.; Daly, K.A.; Jiang, H.; Medberry, C.J.; Tottey, S.; Turner, N.J.; Badylak, S.F. The Effect of Source Animal Age upon the in Vivo Remodeling Characteristics of an Extracellular Matrix Scaffold. *Biomaterials* **2012**, *33*, doi:10.1016/j.biomaterials.2012.04.017.

77. Galindo-Moreno, P.; Abril-García, D.; Carrillo-Galvez, A.B.; Zurita, F.; Martín-Morales, N.; O'Valle, F.; Padial-Molina, M. Maxillary Sinus Floor Augmentation Comparing Bovine versus Porcine Bone Xenografts Mixed with Autogenous Bone Graft. A Split-Mouth Randomized Controlled Trial. *Clin Oral Implants Res* **2022**, *33*, doi:10.1111/clr.13912.

78. Keane, T.J.; Badylak, S.F. The Host Response to Allogeneic and Xenogeneic Biological Scaffold Materials. *J Tissue Eng Regen Med* **2015**, *9*, 504–511, doi:10.1002/term.1874.

79. Sheehy, E.J.; Lemoine, M.; Clarke, D.; Vazquez, A.G.; O'Brien, F.J. The Incorporation of Marine Coral Microparticles into Collagen-Based Scaffolds Promotes Osteogenesis of Human Mesenchymal Stromal Cells via Calcium Ion Signalling. *Mar Drugs* **2020**, *18*, doi:10.3390/md18020074.

80. Carson, M.; Clarke, S. Bioactive Compounds from Marine Organisms: Potential for Bone Growth and Healing. *Mar Drugs* **2018**, *16*, 340, doi:10.3390/md16090340.

81. Iovene, A.; Zhao, Y.; Wang, S.; Amoako, K. Bioactive Polymeric Materials for the Advancement of Regenerative Medicine. *J Funct Biomater* **2021**, *12*, doi:10.3390/jfb12010014.

82. Donnaloja, F.; Jacchetti, E.; Soncini, M.; Raimondi, M.T. Natural and Synthetic Polymers for Bone Scaffolds Optimization. *Polymers (Basel)* **2020**, *12*, 905, doi:10.3390/polym12040905.

83. Rajpoot, K.; Safavi, M.; Sreeharsha, N.; Tekade, R.K. Recent Advances in Regenerative Medicine. In *The Future of Pharmaceutical Product Development and Research*; Elsevier, **2020**; pp. 367–412.

84. Alvarez Echazú, M.I.; Perna, O.; Olivetti, C.E.; Antezana, P.E.; Municoy, S.; Tuttolomondo, M. V.; Galdopórpora, J.M.; Alvarez, G.S.; Olmedo,

D.G.; Desimone, M.F. Recent Advances in Synthetic and Natural Biomaterials-Based Therapy for Bone Defects. *Macromol Biosci* **2022**, *22*, 2100383, doi:10.1002/mabi.202100383.

85. Guo, L.; Liang, Z.; Yang, L.; Du, W.; Yu, T.; Tang, H.; Li, C.; Qiu, H. The Role of Natural Polymers in Bone Tissue Engineering. *J Control Release* **2021**, *338*, doi:10.1016/j.jconrel.2021.08.055.

86. Fan, J.; Abedi-Dorcheh, K.; Sadat Vaziri, A.; Kazemi-Aghdam, F.; Rafieyan, S.; Sohrabinejad, M.; Ghorbani, M.; Rastegar Adib, F.; Ghasemi, Z.; Klavins, K.; et al. A Review of Recent Advances in Natural Polymer-Based Scaffolds for Musculoskeletal Tissue Engineering. *Polymers (Basel)* **2022**, *14*, 2097, doi:10.3390/polym14102097.

87. Bianchi, S.; Mancini, L.; Torge, D.; Cristiano, L.; Mattei, A.; Varvara, G.; Macchiarelli, G.; Marchetti, E.; Bernardi, S. Bio-Morphological Reaction of Human Periodontal Ligament Fibroblasts to Different Types of Dentinal Derivates: In Vitro Study. *Int. J. Mol. Sci* **2021**, *22*, 8681, doi:10.3390/ijms.

88. Bianchi, S.; Bernardi, S.; Continenza, M.A.; Vincenti, E.; Antonouli, S.; Torge, D.; Macchiarelli, G. Scanning Electron Microscopy Approach for Evaluation of Hair Dyed with Lawsonia Inermis Powder: In Vitro Study . *Int J Morphol* **2020**, *38*, 96–100, doi:10.4067/S0717-95022020000100096.

89. Xiong, J.; Menicanin, D.; Zilm, P.S.; Marino, V.; Bartold, P.M.; Gronthos, S. Investigation of the Cell Surface Proteome of Human Periodontal Ligament Stem Cells. *Stem Cells Int* **2016**, *2016*, doi:10.1155/2016/1947157.

90. Minetti, E.; Berardini, M.; Trisi, P. A New Tooth Processing Apparatus Allowing to Obtain Dentin Grafts for Bone Augmentation: The Tooth Transformer. *Open Dent J* **2019**, *13*, 6–14, doi:10.2174/1874210601913010006.

91. Bernardi, S.; Mummolo, S.; Varvara, G.; Marchetti, E.; Continenza, M.A.; Marzo, G.; Macchiarelli, G. Bio-Morphological Evaluation of Periodontal Ligament Fibroblasts on Mineralized Dentin Graft: An in Vitro Study. *J Biol Regul Homeost Agents* **2019**, *33*.

92. Murakami, Y.; Kojima, T.; Nagasawa, T.; Kobayashi, H.; Ishikawa, I. Novel Isolation of Alkaline Phosphatase-Positive Subpopulation from Periodontal Ligament Fibroblasts. *J Periodontol* **2003**, *74*, 780–786, doi:10.1902/jop.2003.74.6.780.

93. Takashiba, S.; Naruishi, K.; Murayama, Y. Perspective of Cytokine Regulation for Periodontal Treatment: Fibroblast Biology. *J Periodontol* **2003**, *74*, 103–110, doi:10.1902/jop.2003.74.1.103.

94. Nogueira, L.S.; Vasconcelos, C.P.; Mitre, G.P.; Bittencourt, L.O.; Plaça, J.R.; Kataoka, M.S. da S.; Pinheiro, J. de J.V.; Garlet, G.P.; De Oliveira, E.H.C.; Lima, R.R. Gene Expression Profile in Immortalized Human

Periodontal Ligament Fibroblasts Through HTERT Ectopic Expression: Transcriptome and Bioinformatic Analysis. *Front Mol Biosci* **2021**, *8*, doi:10.3389/fmolb.2021.679548.

95. Sun, J.; Hu, Y.; Fu, Y.; Zou, D.; Lu, J.; Lyu, C. Emerging Roles of Platelet Concentrates and Platelet-Derived Extracellular Vesicles in Regenerative Periodontology and Implant Dentistry. *APL Bioeng* **2022**, *6*, 031503, doi:10.1063/5.0099872.

96. Anfossi, G.; Trovati, M.; Mularoni, E.; Massucco, P.; Calcamuggi, G.; Emanuelli, G. Influence of Propranolol on Platelet Aggregation and Thromboxane B2 Production from Platelet-Rich Plasma and Whole Blood. *Prostaglandins Leukot Essent Fatty Acids* **1989**, *36*, doi:10.1016/0952-3278(89)90154-3.

97. Mazor, Z.; Horowitz, R.; Prasad, H.; Kotsakis, G. Healing Dynamics Following Alveolar Ridge Preservation with Autologous Tooth Structure. *Int J Periodontics Restorative Dent* **2019**, *39*, doi:10.11607/prd.4138.

98. Annunziata, M.; Guida, L.; Nastri, L.; Piccirillo, A.; Sommese, L.; Napoli, C. The Role of Autologous Platelet Concentrates in Alveolar Socket Preservation: A Systematic Review. *Transfus Med Hemother* **2018**, *45*, 195–203, doi:10.1159/000488061.

99. Mijiritsky, E.; Assaf, H.D.; Kolerman, R.; Mangani, L.; Ivanova, V.; Zlatev, S. Autologous Platelet Concentrates (APCs) for Hard Tissue Regeneration in Oral Implantology, Sinus Floor Elevation, Peri-Implantitis, Socket Preservation, and Medication-Related Osteonecrosis of the Jaw (MRONJ): A Literature Review. *Biology (Basel)* **2022**, *11*, 1254, doi:10.3390/biology11091254.

100. Kobayashi, E.; Flückiger, L.; Fujioka-Kobayashi, M.; Sawada, K.; Sculean, A.; Schaller, B.; Miron, R.J. Comparative Release of Growth Factors from PRP, PRF, and Advanced-PRF. *Clin Oral Investig* **2016**, *20*, doi:10.1007/s00784-016-1719-1.

101. del Corso, M.; Sammartino, G.; Dohan Ehrenfest, D.M. Letter to the Editor: Re: "Clinical Evaluation of a Modified Coronally Advanced Flap Alone or in Combination With a Platelet-Rich Fibrin Membrane for the Treatment of Adjacent Multiple Gingival Recessions: A 6-Month Study." *J Periodontol* **2009**, *80*, doi:10.1902/jop.2009.090253.

102. Sharma, A.; Pradeep, A.R. Autologous Platelet-Rich Fibrin in the Treatment of Mandibular Degree II Furcation Defects: A Randomized Clinical Trial. *J Periodontol* **2011**, *82*, doi:10.1902/jop.2011.100731.

103. Masuki, H.; Okudera, T.; Watanebe, T.; Suzuki, M.; Nishiyama, K.; Okudera, H.; Nakata, K.; Uematsu, K.; Su, C.-Y.; Kawase, T. Growth Factor and Pro-Inflammatory Cytokine Contents in Platelet-Rich Plasma (PRP), Plasma Rich in Growth Factors (PRGF), Advanced Platelet-Rich Fibrin (A-

PRF), and Concentrated Growth Factors (CGF). *Int J Implant Dent* **2016**, *2*, doi:10.1186/s40729-016-0052-4.

104. Everts, P.A.M.; Hoffmann, J.; Weibrich, G.; Mahoney, C.B.; Schönberger, J.P.A.M.; van Zundert, A.; Knape, J.T.A. Differences in Platelet Growth Factor Release and Leucocyte Kinetics during Autologous Platelet Gel Formation. *Transfus Med* **2006**, *16*, doi:10.1111/j.1365-3148.2006.00708.x.

105. Waters, J.H.; Roberts, K.C. Database Review of Possible Factors Influencing Point-of-Care Platelet Gel Manufacture. *J Extra Corpor Technol* **2004**, *36*.

106. CharrierJ-B; Monteil, J.P.; Albert, S.; Collon, S.; Bobin, S.; Dohan Ehrenfest, D.M. Relevance of Choukroun's Platelet-Rich Fibrin (PRF) and SMAS Flap in Primary Reconstruction after Superficial or Subtotal Parotidectomy in Patients with Focal Pleiomorphic Adenoma: A New Technique. *Rev Laryngol Otol Rhinol (Bord)* **2008**, *129*.

107. Smithmyer, M.E.; Sawicki, L.A.; Kloxin, A.M. Hydrogel Scaffolds as *in Vitro* Models to Study Fibroblast Activation in Wound Healing and Disease. *Biomater. Sci.* **2014**, *2*, 634–650, doi:10.1039/C3BM60319A.

108. Bianchi, S.; Macchiarelli, G.; Micara, G.; Linari, A.; Boninsegna, C.; Aragona, C.; Rossi, G.; Cecconi, S.; Nottola, S.A. Ultrastructural Markers of Quality Are Impaired in Human Metaphase II Aged Oocytes: A Comparison between Reproductive and in Vitro Aging. *J Assist Reprod Genet* **2015**, *32*, 1343–1358, doi:10.1007/s10815-015-0552-9.

109. Shakhov, A.S.; Kovaleva, P.A.; Churkina, A.S.; Kireev, I.I.; Alieva, I.B. Colocalization Analysis of Cytoplasmic Actin Isoforms Distribution in Endothelial Cells. *Biomedicines* **2022**, *10*, doi:10.3390/biomedicines10123194.

110. Bianchi, S.; Macchiarelli, G.; Micara, G.; Aragona, C.; Maione, M.; Nottola, S.A. Ultrastructural and Morphometric Evaluation of Aged Cumulus-Oocyte- Complexes. *It J Anat Embryol* **2013**, *118*.

111. Giusti, I.; Bianchi, S.; Nottola, S.A.; Macchiarelli, G.; Dolo, V. Clinical Electron Microscopy in the Study of Human Ovarian Tissues. *EMBJ* **2019**, *14*, 145–151, doi:10.3269/1970-5492.2019.14.34.

112. Cooper, G.M. Structure and Organization of Actin Filaments. *The Cell: A Molecular Approach. 2nd edition.* **2000**.

113. Pitzurra, L.; Jansen, I.D.C.; de Vries, T.J.; Hoogenkamp, M.A.; Loos, B.G. Effects of L-PRF and A-PRF+ on Periodontal Fibroblasts in in Vitro Wound Healing Experiments. *J Periodontal Res* **2020**, *55*, doi:10.1111/jre.12714.

114. Bornfeldt, K.E.; Raines, E.W.; Graves, L.M.; Skinner, M.P.; Krebs, E.G.; Ross, R. Platelet-derived Growth Factor: Distinct Signal Transduction

Pathways Associated with Migration versus Proliferation. *Ann N Y Acad Sci* **1995**, *766*, doi:10.1111/j.1749-6632.1995.tb26691.x.

115. Tsay, R.C.; Vo, J.; Burke, A.; Eisig, S.B.; Lu, H.H.; Landesberg, R. Differential Growth Factor Retention by Platelet-Rich Plasma Composites. *J Oral Maxillofac Surg* **2005**, *63*, doi:10.1016/j.joms.2004.09.012.

116. Zhang, S.; Li, X.; Qi, Y.; Ma, X.; Qiao, S.; Cai, H.; Zhao, B.C.; Jiang, H.B.; Lee, E.-S. Comparison of Autogenous Tooth Materials and Other Bone Grafts. *Tissue Eng Regen Med* **2021**, *18*, 327–341, doi:10.1007/s13770-021-00333-4.

117. Yüceer-Çetiner, E.; Özkan, N.; Önger, M.E. Effect of Autogenous Dentin Graft on New Bone Formation. *J Craniofac Surg* **2021**, *32*, doi:10.1097/SCS.0000000000007403.

118. Solomon, S.M.; Timpu, D.; Forna, D.A.; Stefanache, M.A.M.; Martu, S.; Stoleriu, S. AFM Comparative Study of Root Surface Morphology after Three Methods of Scaling. *Materiale Plastice* **2016**, *53*.

119. Martu, M.A.; Surlin, P.; Lazar, L.; Maftei, G.A.; Luchian, I.; Gheorghe, D.N.; Rezus, E.; Toma, V.; Foia, L.G. Evaluation of Oxidative Stress before and after Using Laser and Photoactivation Therapy as Adjuvant of Non-Surgical Periodontal Treatment in Patients with Rheumatoid Arthritis. *Antioxidants* **2021**, *10*, doi:10.3390/antiox10020226.

120. Santos, A.; Botelho, J.; Machado, V.; Borrecho, G.; Proença, L.; Mendes, J.J.; Mascarenhas, P.; Alcoforado, G. Autogenous Mineralized Dentin versus Xenograft Granules in Ridge Preservation for Delayed Implantation in Post-Extraction Sites: A Randomized Controlled Clinical Trial with an 18 Months Follow-Up. *Clin Oral Implants Res* **2021**, *32*, doi:10.1111/clr.13765.

121. Minetti, E.; Palermo, A.; Savadori, P.; Barlattani, A.; Franco, R.; Michele, M.; Gianfreda, F.; Bollero, P. Autologous Tooth Graft: A Histological Comparison between Dentin Mixed with Xenograft and Dentin Alone Grafts in Socket Preservation. *J Biol Regul Homeost Agents* **2019**, *33*.

122. Yeomans, J.D.; Urist, M.R. Bone Induction by Decalcified Dentine Implanted into Oral, Osseous and Muscle Tissues. *Arch Oral Biol* **1967**, *12*, doi:10.1016/0003-9969(67)90095-7.

123. Bessho, K.; Tanaka, N.; Matsumoto, J.; Tagawa, T.; Murata, M. Human Dentin-Matrix-Derived Bone Morphogenetic Protein. *J Dent Res* **1991**, *70*, doi:10.1177/00220345910700030301.

124. Blum, B.; Moseley, J.; Miller, L.; Richelsoph, K.; Haggard, W. Measurement of Bone Morphogenetic Proteins and Other Growth Factors in Demineralized Bone Matrix. *Orthopedics* **2004**, *27*, doi:10.3928/0147-7447-20040102-17.

125. Kasaj, A.; Willershausen, B.; Junker, R.; Stratul, S.I.; Schmidt, M. Human Periodontal Ligament Fibroblasts Stimulated by Nanocrystalline Hydroxyapatite Paste or Enamel Matrix Derivative. An in Vitro Assessment of PDL Attachment, Migration, and Proliferation. *Clin Oral Investig* **2012**, *16*, doi:10.1007/s00784-011-0570-7.

126. Kasaj, A.; Klein, M.O.; Dupont, J.; Willershausen, B.; Krahn, U.; Götz, H.; Zeiler, J.; Brüllmann, D.; Duschner, H. Early Root Surface Colonization by Human Periodontal Ligament Fibroblasts Following Treatment with Different Biomaterials. *Acta Odontol Scand* **2013**, *71*, doi:10.3109/00016357.2013.777115.

127. Alliot-Licht, B.; de Lange, G.L.; Gregoire, M. Effects of Hydroxyapatite Particles on Periodontal Ligament Fibroblast-Like Cell Behavior. *J Periodontol* **1997**, *68*, doi:10.1902/jop.1997.68.2.158.

128. Tabatabaei, F.S.; Tatari, S.; Samadi, R.; Torshabi, M. Surface Characterization and Biological Properties of Regular Dentin, Demineralized Dentin, and Deproteinized Dentin. *J Mater Sci Mater Med* **2016**, *27*, doi:10.1007/s10856-016-5780-8.

129. Echavidre, W.; Picco, V.; Faraggi, M.; Montemagno, C. Integrin-Avβ3 as a Therapeutic Target in Glioblastoma: Back to the Future? *Pharmaceutics* **2022**, *14*, 1053, doi:10.3390/pharmaceutics14051053.

130. Pang, X.; He, X.; Qiu, Z.; Zhang, H.; Xie, R.; Liu, Z.; Gu, Y.; Zhao, N.; Xiang, Q.; Cui, Y. Targeting Integrin Pathways: Mechanisms and Advances in Therapy. *Signal Transduct Target Ther* **2023**, *8*, 1, doi:10.1038/s41392-022-01259-6.

131. Virtanen, J.A.; Vartiainen, M.K. Diverse Functions for Different Forms of Nuclear Actin. *Curr Opin Cell Biol* **2017**, *46*, 33–38, doi:10.1016/j.ceb.2016.12.004.

132. Barczyk, M.; Bolstad, A.I.; Gullberg, D. Role Of Integrins In The Periodontal Ligament: Organizers And Facilitators. *Periodontol 2000* **2013**, *63*, doi:10.1111/prd.12027.

133. Hamilton, D.W.; Oates, C.J.; Hasanzadeh, A.; Mittler, S. Migration of Periodontal Ligament Fibroblasts on Nanometric Topographical Patterns: Influence of Filopodia and Focal Adhesions on Contact Guidance. *PLoS One* **2010**, *5*, doi:10.1371/journal.pone.0015129.

134. Hakkinen, K.M.; Harunaga, J.S.; Doyle, A.D.; Yamada, K.M. Direct Comparisons of the Morphology, Migration, Cell Adhesions, and Actin Cytoskeleton of Fibroblasts in Four Different Three-Dimensional Extracellular Matrices. *Tissue Eng Part A* **2011**, *17*, doi:10.1089/ten.tea.2010.0273.

135. Amini, A.R.; Laurencin, C.T.; Nukavarapu, S.P. Bone Tissue Engineering: Recent Advances and Challenges. *Crit Rev Biomed Eng* **2012**, *40*, doi:10.1615/CritRevBiomedEng.v40.i5.10.

136. Prieto, E.M.; Talley, A.D.; Gould, N.R.; Zienkiewicz, K.J.; Drapeau, S.J.; Kalpakci, K.N.; Guelcher, S.A. Effects of Particle Size and Porosity on in Vivo Remodeling of Settable Allograft Bone/Polymer Composites. *J Biomed Mater Res B Appl Biomater* **2015**, *103*, doi:10.1002/jbm.b.33349.

137. Klüppel, L.E.; Antonini, F.; Olate, S.; Nascimento, F.F.; Albergaria-Barbosa, J.R.; Mazzonetto, R. Bone Repair Is Influenced by Different Particle Sizes of Anorganic Bovine Bone Matrix: A Histologic and Radiographic Study in Vivo. *J Craniofac Surg* **2013**, *24*, doi:10.1097/SCS.0b013e318286a0a3.

138. Leiblein, M.; Koch, E.; Winkenbach, A.; Schaible, A.; Nau, C.; Büchner, H.; Schröder, K.; Marzi, I.; Henrich, D. Size Matters: Effect of Granule Size of the Bone Graft Substitute (Herafill®) on Bone Healing Using Masquelet's Induced Membrane in a Critical Size Defect Model in the Rat's Femur. *J Biomed Mater Res B Appl Biomater* **2020**, *108*, doi:10.1002/jbm.b.34495.

139. Roberts, T.T.; Rosenbaum, A.J. Bone Grafts, Bone Substitutes and Orthobiologics the Bridge between Basic Science and Clinical Advancements in Fracture Healing. *Organogenesis* **2012**, *8*, doi:10.4161/org.23306.

140. Mazzoni, S.; Mohammadi, S.; Tromba, G.; Diomede, F.; Piattelli, A.; Trubiani, O.; Giuliani, A. Role of Cortico-Cancellous Heterologous Bone in Human Periodontal Ligament Stem Cell Xeno-Free Culture Studied by Synchrotron Radiation Phase-Contrast Microtomography. *Int J Mol Sci* **2017**, *18*, doi:10.3390/ijms18020364.

141. Conz, M.B.; Granjeiro, J.M.; Soares, G. de A. Hydroxyapatite Crystallinity Does Not Affect the Repair of Critical Size Bone Defects. *J Appl Oral Sci* **2011**, *19*, doi:10.1590/S1678-77572011005000007.

142. Fernández, M.P.R.; Gehrke, S.A.; Martinez, C.P.A.; Guirado, J.L.C.; de Aza, P.N. SEM-EDX Study of the Degradation Process of Two Xenograft Materials Used in Sinus Lift Procedures. *Materials* **2017**, *10*, doi:10.3390/ma10050542.

143. Block, M.S. Does the Use of High-Temperature–Processed Xenografts for Ridge Augmentation Result in Ridge Width Stability Over Time? *J Oral Maxillofac Surg* **2020**, *78*, doi:10.1016/j.joms.2020.06.004.

144. Gehrke, S.A.; Mazón, P.; Pérez-Díaz, L.; Calvo-Guirado, J.L.; Velásquez, P.; Aragoneses, J.M.; Fernández-Domínguez, M.; de Aza, P.N. Study of Two Bovine Bone Blocks (Sintered and Non-Sintered) Used for Bone Grafts: Physico-Chemical Characterization and in Vitro Bioactivity and Cellular Analysis. *Materials* **2019**, *12*, doi:10.3390/ma12030452.

145. World Health Organization WHO Infection Control Guidelines for Transmissible Spongiform Encephalopathies Report of a WHO Consultation. *World Health Organization* **2000**.

146. Lei, P.; Sun, R.; Wang, L.; Zhou, J.; Wan, L.; Zhou, T.; Hu, Y. A New Method for Xenogeneic Bone Graft Deproteinization: Comparative Study of Radius Defects in a Rabbit Model. *PLoS One* **2015**, *10*, doi:10.1371/journal.pone.0146005.

147. Bi, L.; Li, D.C.; Huang, Z.S.; Yuan, Z. Effects of Sodium Hydroxide, Sodium Hypochlorite, and Gaseous Hydrogen Peroxide on the Natural Properties of Cancellous Bone. *Artif Organs* **2013**, *37*, doi:10.1111/aor.12048.

Appendix

List of articles and abstracts produced during the PhD Course.

Full – lenght papers

- **Scanning Electron Microscopy Approach for Evaluation of Hair Dyed with Lawsonia Inermis Powder: In Vitro Study.**

  Bianchi, S.; Bernardi, S.; Continenza, M.A.; Vincenti, E.; Antonouli, S.; Torge, D.; Macchiarelli, G. *Int. J. Morphol.* **2020**, 38, 96-100; DOI:10.4067/S0717-95022020000100096

  Summary: This study investigates the morphological reaction of hair to the herbal dye derived from Lawsonia inermis. SEM was applied to evaluate dyed hair qualitatively and quantitatively when compared to undyed hair. The results showed a positive reaction on the cuticula pattern and on the diameters of the selected samples after henna treatment.

- **Association between female reproductive health and mancozeb: Systematic review of experimental models.**

  Bianchi, S.; Nottola, S.A.; Torge, D.; Palmerini, M.G.; Necozione, S.; Macchiarelli, G. *Int. J. Environ. Res. Public Health.* **2020**, 7 7,2580. https://doi.org/10.3390/ijerphl7072580

  Summary: This systematic review summarizes current evidence on mancozeb exposure and female reproductive disease. The database search identified 250 scientific articles, 20 of which met our inclusion criteria. Selected data then reviewed and summarized in tables, highlighting how mancozeb represents an epigenetic hazard for female reproductive health.

- **Evaluation of Different Autologous Platelet Concentrate Biomaterials: Morphological and Biological Comparisons and Considerations.**

  Marchetti, E.; Mancini, L.; Bernardi, S.; Bianchi, S.; Cristiano, L.; Torge, D.; Marzo, G.; Macchiarelli, G. *Materials.* **2020**, *13,* 2282. https://doi.org/10.3390/ma13102282

- **Platelets' Role in Dentistry: From Oral Pathology to Regenerative Potential.**

  Bianchi, S.; Torge, D.; Rinaldi, F.; Piattelli, M.; Bernardi, S.; Varvara, G. *Biomedicines.* **2022, /** *0,* 218. https://doi.org/10.3390/biomedicinesl00202l8.

- **Bio - morphological reaction of human periodontal ligament fibroblasts to different types of dentinal derivates: in vitro study.**

  Bianchi, S.; Mancini, L.; Torge, D.; Cristiano, L.; Mattei, A.; Varvara, G.; Macchiarelli, G.; Marchetti, E.; Bernardi, S. *Int. J. Mol. Sci.* **2021,** *22,* 8681. https://doi.ore/10.3390/ijms22l6868l

- **Histopathological Features of SARS-CoV-2 in Extrapulmonary Organ Infection: A Systematic Review of Literature.**

  Torge, D.; Bernardi, S.; Arcangeli, M.; Bianchi, S. *Pathogens*. **2022**, *11*, 867. https://doi.org/10.3390/pathogens11080867

  Summary: This systematic review summarizes the most recent histopathological evidence on COVID-19 structural and ultrastructural alterations in extra – pulmonary tissues and organs. Thirty – one articles were included in this systematic review, highlighting how COVID-19 induces, at histopathological level, detrimental effects on tissues, with significant degenerative dynamics.

- **Effect of temperature on transfer of *Midichloria*-like organism and development of red mark syndrome in rainbow trout (*Oncorhynchus mykiss*).**

  Orioles, M.; Galeotti, M.; Saccà, E.; Bulfoni, M.; Corazzin, M.; Bianchi, S.; Torge, D.; Macchiarelli, G.; Magi, G.E.; Schmidt, J.G. *Aquaculture* **2022**, *560*. doi:10.1016/j.aquaculture.2022.738577

  Summary: This study investigates the RMS progression at different temperatures. PCR and digital droplet PCR were applied to define pathogen load, in spleen and skin samples of rainbow trout, affected by RMS. Furthermore, RMS lesions were described by macroscopic and histological scoring. Finally, TEM was applied to localize MLOs on spleen and skin samples derived from rainbow trouts, affected by RMS.

- **Morphological and Biological Evaluations of Human Periodontal Ligament Fibroblasts in Contact with Different Bovine Bone Grafts Treated with Low-Temperature Deproteinisation Protocol.**

  Bianchi, S.; Bernardi, S.; Mattei, A.; Cristiano, L.; Mancini, L.; Torge, D.; Varvara, G.; Macchiarelli, G.; Marchetti, E. *Int. J. Mol. Sci.* **2022**, *23*, 5273. https://doi.org/10.3390/ijms23095273

- **Proliferation and Morphological Assessment of Human Periodontal Ligament Fibroblast towards Bovine Pericardium Membranes: An In Vitro Study.**

  Bianchi, S.; Bernardi, S.; Simeone, D.; Torge, D.; Macchiarelli, G.; Marchetti, E. *Materials* **2022**, *15*, 8284. https://doi.org/10.3390/ma15238284

  Summary: This study aims to investigate the proliferation abilities and the attachment of hPLFs over two bovine pericardium membranes with different thicknesses, 0.2 mm, and 0.4 mm, respectively. Biological response was evaluated by XTT assays, while morphological reactions were described by LM, and SEM.

  Our results highlighted a similar cell behavior towards the two bovine pericardium membranes, detecting a cellular migration along and within the layers of the membrane, with binding to membrane fibers by means of filopodial extensions.

ABSTRACT IN CONFERENCE PROCEEDINGS

- **Autologous biomaterials in dentistry: role of platelets derivated, morphological and clinical consideration.**

  Bernardi, S.; Torge, D.; Macchiarelli, G.; Bianchi, S. In: **"Morfologia e dintorni"** 3° Incontro Nazionale, **26 Settembre 2020.**

ABSTRACT ON JOURNAL

- **Morphological behaviour of human periodontal ligament fibroblasts towards the exposition to dentinal derivates biomaterial.**

  Bernardi, S., Bianchi, S., Torge, D., Macchiarelli, G. *Ital J Anat Embr*. **2021,** 125 (1s), 45.

- **Evaluation of Proliferation and Morphological features of Human Periodontal Ligament Fibroblasts in Contact with Different Bovine Bone Grafts Treated with Low Temperature Deproteinisation Protocol.**

  Torge, D., Bernardi, S., Bianchi, S., Macchiarelli, G. *Ital J Anat Embr*. **2022**, 126 (1s), 212.

Seminars and webinars

- "Navigating scientific literature skills: reading and understanding scientific papers". Prof. Giuseppe Di Giovanni - seminar, 21 November 2019 (16:30 - 18:30), L'Aquila.
- "Presentation skills: how to give effective talks". Prof. Giuseppe Di Giovanni - seminar, 25 November 2019 (16:30 - 18:30), L'Aquila.
- "Fund raising skills: understanding funding opportunities for young scientists and understanding the basics of a successful proposal". Prof. Giuseppe Di Giovanni - seminar, 3 December 2019 (16:30 - 18:30), L'Aquila.
- "L'Adesione cellulare: aspetti molecolari e rilevanza clinica". Dott.ssa Paola Fortugno e Prof. Mauro Bologna – seminar, 4 December 2019 (11:00 - 13:00), L'Aquila.
- "Call Green Deal di Horizon 2020". Dott.ssa Miriam De Angelis – training course Agenzia Promozione Ricerca Europea (APRE), 29 October 2020 (10:00 - 12:30), L'Aquila.
- "Valorizzazione dei risultati della ricerca". Prof. Luciano Fratocchi, Dott. Marco De Luca - seminario, 14 December 2020 (14:30 - 18:30), L'Aquila.
- "Finanziamenti alla ricerca: quali opportunità per i giovani?". Comitato «Amici dell'Anatomia» - seminar, 30 January 2021 (10:00 - 11:30), L'Aquila.
- "Laurea, Ph. D. e poi?". Prof. Armando Carlone - seminar, 19 February 2021 (10:00 - 12:00), L'Aquila.
- "CV, cover letter e colloquio". Prof. Armando Carlone - seminar, 19 February 2021 (10:00 - 12:00), L'Aquila.

- “Il chimico in azienda...ma non solo”. Prof. Armando Carlone - seminar, 22 February 2021 (10:00 - 12:00), L’Aquila.
- “Protezione, creatività e proprietà intellettuale - II parte”. Avv. Francesca Retko - seminar, 12 April 2021 (9:00 - 13:00/14:30 - 16:30), L’Aquila.
- “Start-up e spin-off - I parte”. Prof. Luciano Fratocchi, Dott. Emesto Finocchi, Dott. Giulio Giorgi, Dott. Massimo Parisse - seminar, 17 May 2021 (9:00 - 13:00/ 14:30 - 16:30), L’Aquila.
- “Start-up e spin-off - II parte”. Prof. Luciano Fratocchi, Dott. Ernesto Finocchi, Dott. Giulio Giorgi, Dott. Massimo Parisse - seminar, 25 June 2021 (9:00 - 13:00/14:30 - 16:30), L’Aquila.
- “Nanoinnovation Conference & Exhibition 2021”. Online Congress, 21 - 24 September 2021 (11:00 – 13:00/14:00 – 15:30), Roma.
- “La ricerca collaborativa in Horizon Europe: come scrivere una proposta di successo”. Dott.ssa Miriam De Angelis – Training Course Agenzia Promozione Ricerca Europea (APRE), 10 December 2021 (9:00 – 13:15), L’Aquila.
- “Sectra Education Portal Initial Training”. Dr. Henrik Gadde – Training Course, 19 January 2022 (9:00 - 13:00), L’Aquila.
- “Sectra Training - Part 1”. Dr. Henrik Gadde - Training Course, 25 January 2022 (9:00 -11:00), L’Aquila.
- “Sectra Training - Part 2”. Dr. Henrik Gadde - Training Course, 26 January 2022 (9:00 - 11:00), L’Aquila.
- “Sectra Education Portal Training”. Dr. Henrik Gadde – Training Course, 25 May 2022 (10:00 – 11:30), L’Aquila.
- “Immune system in chronic pain plasticity”. Prof.ssa Anna Maria Cimini, Prof. Livio Luongo - seminar, 25 October 2022 (14:30 -15:30), L’Aquila.

- “Forebrain pain mechanisms: beyond the pain matrix”. Prof.ssa Anna Maria Cimini, Prof. Sabatino Maione - seminar, 25 October 2022 (15:30 - 16:30), L’Aquila.
- “La Terra dei Fuochi tra inquinamento antropico e naturale”. Prof.ssa Maria Grazia Cifone, Dott. Adriano Pistilli - seminar, 4 November 2022 (11:00 -13:00), L’Aquila.
- “The impact of pain on human life: how to relieve human suffering”. Prof.ssa Anna Maria Cimini, Prof. Carmelo Scarpignato - seminar, 30 November 2022 (14:30 - 16:30), L’Aquila.
- “Come scrivere una proposta di successo nel tema eic –accelerator”. Dott. Renato Fa – Training Course Agenzia Promozione Ricerca Europea (APRE), 1 December 2022 (9:30 - 12:00), L’Aquila.
- “Come scrivere una proposta di successo nel tema eic –pathfinder – eic transition -ca & ipr”. Dott.ssa Stefania Marassi, Dott.ssa Valentina Fioroni – Training Course Agenzia Promozione Ricerca Europea (APRE), 2 December 2022 (9:00 - 11:45), L’Aquila.